JCI The Journal of Clinical Investigation

The secreted micropeptide C4orf48 enhances renal fibrosis via an RNA-binding mechanism

Jiayi Yang, … , David J. Nikolic-Paterson, Xueqing Yu

J Clin Invest. 2024. https://doi.org/10.1172/JCI178392.

Research In-Press Preview **Nephrology**

Graphical abstract

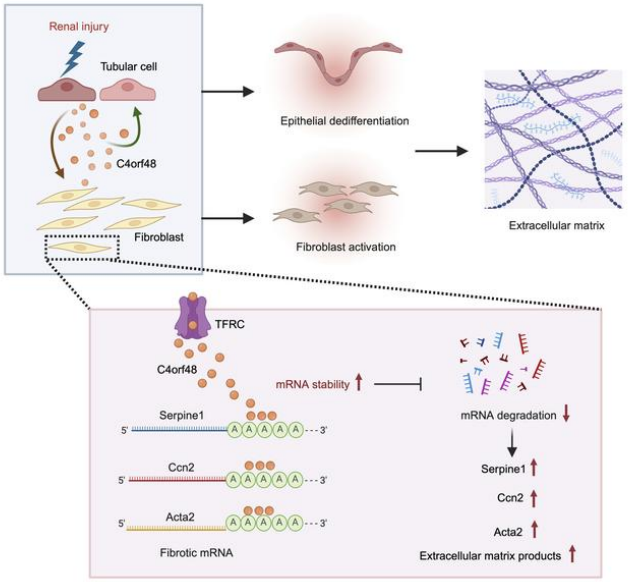

Title: The secreted micropeptide C4orf48 enhances renal fibrosis via an RNA-binding mechanism.

One Sentence Summary:

C4orf48 is an RNA-binding peptide that enhances renal fibrosis.

Authors: Jiayi Yang[1,2†], Hongjie Zhuang[3†], Jinhua Li[4,5,6,7†*], Ana B. Nunez-Nescolarde[8], Ning Luo[1,2], Huiting Chen[6], Andy Li[7], Xinli Qu[8], Qing Wang[4,5], Jinjin Fan[1,2], Xiaoyan Bai[4,5], Zhiming Ye[4,5], Bing Gu[9], Yue Meng[9], Xingyuan Zhang[10], Di Wu[10], Youyang Sia[11], Xiaoyun Jiang[3], Wei Chen[1,2], Alexander N. Combes[8], David J. Nikolic-Paterson[7], Xueqing Yu[4,5*]

Affiliations:

[1]Department of Nephrology, The First Affiliated Hospital, Sun Yat-sen University; 58th Zhongshan Road II, Guangzhou, 510080, China.

[2]Key Laboratory of Nephrology, National Health Commission and Guangdong Province; Guangzhou, 510080, China.

[3]Department of Paediatrics, The First Affiliated Hospital, Sun Yat-sen University; Guangzhou, China.

[4]Department of Nephrology, Guangdong Provincial People's Hospital and Guangdong Academy of Medical Sciences; Guangzhou, China.

[5]Guangdong-Hong Kong Joint Laboratory on Immunological and Genetic Kidney Diseases, Guangdong Provincial People's Hospital and Guangdong Academy of Medical Sciences; Guangzhou, China.

[6]The Second Clinical College, Guangdong Medical University; Dongguan, Guangdong, 528399, China.

[7]Department of Nephrology, Monash Health and Monash University Department of Medicine; Clayton, Victoria, 3168, Australia.

[8]Department of Anatomy and Developmental Biology, Monash Biomedicine Discovery Institute, Monash University; Clayton, Victoria, 3800, Australia.

[9]Department of Clinical Laboratory, Guangdong Provincial People's Hospital and Guangdong Academy of Medical Sciences; Guangzhou, China.

[10]Department of Biostatistics, UNC Gillings School of Global Public Health, University of North Carolina, Chapel Hill, NC 27599-7455, USA

[11]School of Life Science, Tsinghua University, Beijing, 100084, China

[†]Authors contributed equally to this work.

*Correspondence should be addressed to Jinhua Li (lijinhua@gdph.org.cn) or Xueqing Yu (yuxueqing@gdph.org.cn).

Jinhua Li, MBBS, PhD

Department of Nephrology

Guangdong Provincial People's Hospital, Guangdong Academy of Medical Science, Guangzhou, 510080, China

E-mail: lijinhua@gdph.org.cn

Xueqing Yu, MD, PhD

Department of Nephrology

Guangdong Provincial People's Hospital, Guangdong Academy of Medical Science,

Guangzhou, 510080, China

E-mail: yuxueqing@gdph.org.cn

Abstract

Renal interstitial fibrosis is an important mechanism in the progression of chronic kidney disease (CKD) to end-stage kidney disease. However, we lack specific treatments to slow or halt renal fibrosis. Ribosome profiling identified upregulation of a secreted micropeptide, C4orf48 (Cf48), in mouse diabetic nephropathy. *Cf48* RNA and protein levels were upregulated in tubular epithelial cells in human and experimental CKD. Serum Cf48 levels were increased in human CKD and correlated with loss of kidney function, increasing CKD stage, and the degree of active interstitial fibrosis. Cf48 overexpression in mice accelerated renal fibrosis, while *Cf48* gene deletion or knockdown by antisense oligonucleotides significantly reduced renal fibrosis in CKD models. In vitro, recombinant Cf48 (rCf48) enhanced TGF-β1-induced fibrotic responses in renal fibroblasts and epithelial cells independent of Smad3 phosphorylation. Cellular uptake of Cf48 and its pro-fibrotic response in fibroblasts operated via the transferrin receptor. RNA immunoprecipitation-sequencing identified Cf48 binding to mRNA of genes involved in the fibrotic response, including *Serpine1*, *Acta2*, *Ccn2* and *Col4a1*. rCf48 binds to the 3′-untranslated region of *Serpine1* and increases mRNA half-life. We identify the secreted Cf48 micropeptide as a potential enhancer of renal fibrosis which operates as an RNA-binding peptide to promote the production of extracellular matrix.

INTRODUCTION

Approximately 8%–18% of adults suffer from chronic kidney disease (CKD) worldwide in both developed and developing countries (1). Diabetes and hypertension are the two leading causes of CKD (2). Hyperglycemia, hypertension, and albuminuria management, together with sodium/glucose cotransporter 2 inhibitor administration for type 2 diabetes, retard but do not halt the progression to end-stage renal disease (ESRD) (2, 3). Patients with ESRD require kidney replacement therapies, such as dialysis or kidney transplantation, which have a major impact upon patients and their families, as well as a high healthcare costs. This urgent unmet clinical need prompted us to seek new therapeutic targets to suppress renal fibrosis.

Glomerular filtration barrier damage and glomerular hemodynamic alterations are characteristic of most CKD forms. However, injury to the proximal tubular epithelium, which makes up 50% of kidney cells, is also an important driver in the progression of CKD. Cortical interstitial expansion is the best histologic predictor of renal functional decline across all CKD types (4-6). Across multiple cohorts of patients with CKD, urinary levels of KIM1/HAVCR1, which is a specific marker of proximal tubular epithelial cell injury, are highest in patients with reduced kidney function (7). In addition, diabetes-induced proximal tubular cell damage is an early event that both predicts and contributes to the development of diabetic nephropathy (DN) (8, 9). Furthermore, cell maladaptive repair of damaged proximal tubular cells is a key factor in the transition of acute kidney injury (AKI) to CKD (10). Thus,

understanding how proximal tubular cell damage drives the progression CKD may identify new therapeutic targets to target renal fibrosis.

Micropeptides are small proteins of < 100 amino acids which are encoded by small open reading frames (smORF). This class of molecule has been overlooked because smORF often lack features of classical protein coding genes, and a threshold length of 300 nucleotides, or 100 amino acids, was arbitrarily and historically set as a minimum size for ontological studies. However, the importance of micropeptides in regulating physiological and/or pathological processes is now being recognized, such as in embryonic development (11), DNA repair (12), metabolic homeostasis (13), muscle regeneration (14), and cell death (15). However, the existence and biological function of micropeptides in the pathogenesis of CKD is unknown.

The present study used ribosome profiling and bioinformatics analysis to screen a mouse diabetic kidney disease and identified secreted micropeptide C4orf48 (Cf48 for brevity, also known as NICOL1) as a candidate molecule involved in renal fibrosis. Cf48 expression was upregulated in human and mouse CKD models, with serum Cf48 levels inversely correlated with kidney function in human CKD. Transgenic overexpression of Cf48, or *Cf48* gene deletion in mice substantially modulated renal fibrosis in models of streptozotocin (STZ)-induced DN, folic acid (FA)-induced nephropathy, and unilateral ureteral obstruction (UUO). Recombinant Cf48 (rCf48) enhanced transforming growth factor-β1 (TGF-β1)-induced fibrotic responses in renal

fibroblasts and epithelial cells independent of Smad3 activation (phosphorylation). rCf48 binds to, and is taken up into fibroblasts, by the transferrin receptor (TFRC). Mechanistically, Cf48 binds to a large number of RNA species involved in extracellular matrix deposition. For example, Cf48 binds to the 3'-end of *Serpine1* mRNA, causing an increase in mRNA half-life. These data establish that the Cf48 micropeptide acts as a potential enhancer of renal fibrosis via binding to RNA molecules to promote extracellular matrix deposition. Cf48 may be a biomarker of active renal fibrosis and a therapeutic target in CKD.

RESULTS

Identification of Cf48 as a putative profibrotic micropeptide in CKD

Seeking to identify micropeptides involved in renal fibrosis, we used ribosome profiling to screen kidney tissue from *Nos3*$^{-/-}$ mice with streptozotocin (STZ)-induced diabetic nephropathy (DN) – a model of progressive DN (16) – compared to age-matched, non-diabetic *Nos3*$^{-/-}$ control mice (Supplementary Table S1). Differentially expressed ($P < 0.05$ by two-tailed *t*-test) molecules were defined, with a criterion of ≥ 2-fold change between the two groups (Supplementary Table S2). Enrichment analysis identified upregulation of 471 molecules with a putative extracellular localization in DN vs control mice (Supplementary Table S3). After excluding 159 extracellular matrix molecules, 15 micropeptides (≦100 amino acids) were identified from 312 potential candidates. Chemokine ligands (Ccl5, Ccl7, Ccl8, Ccl11, Ccl17, Ccl20, Ccl22, Cxcl1 and Cxcl10), and micropeptides without orthologues in humans (Wfdc15b, Wfdc17) were excluded. The remaining four peptides were Gm1673 (C4orf48 in humans, Cf48), Apoc1, Hilpda, and Tmsb4x. To screen for a profibrotic function, these four peptides were individually overexpressed in the rat renal fibroblast line NRK49F via a retroviral vector. Cf48 overexpression most clearly enhanced TGF-β1-induced upregulation of Acta2 (α-smooth muscle actin, α-SMA), collagen I and fibronectin in comparison to the empty vector (EV) control (Figure 1A). Therefore, Cf48 was investigated as a potential enhancer of the fibrotic response.

A comparison of the Cf48 amino acid sequence shows high conservation between humans and mice, and substantial homology with more distant genera (Supplementary Figure S1A). A signal peptide is predicted in both human and mouse Cf48 (Supplementary Figures S1B and C). To test for secretion of a bioactive peptide, 293T cells were transfected with a Cf48 overexpression plasmid, or empty control plasmid, and conditioned media collected. Mass spectrometry confirmed the presence of Cf48 in Cf48 conditioned media (Supplementary Figure S1D). Conditional media from Cf48 transfected cells substantially enhanced TGF-β1-stimulated expression of Acta2, collagen I, and Serpine1 in NRK49F cells (Figures 1B-D).

Upregulation of Cf48 expression in human and experimental CKD

In contrast to the very low levels of *Cf48* RNA and protein seen in normal mouse kidney, mice with STZ-induced DN showed a very substantial increase in kidney Cf48 RNA and protein levels (Figures 1E–H**)**. Confocal microscopy showed very little staining for Cf48 in normal mouse kidney, but substantial tubular Cf48 staining was evident in mouse DN, with some ACTA2+ myofibroblasts also showing Cf48 staining **(**Figures 1G and H**)**. Increased kidney Cf48 RNA levels and increased Cf48 protein expression in tubular cells (and some myofibroblasts) was also evident in folic acid nephropathy (FA nephropathy): a model of AKI-CKD transition (Figures 1I-K).

In situ hybridization revealed very low Cf48 mRNA levels in normal human kidney, but Cf48 mRNA was markedly increased in tubular epithelial cells, but not

glomerular cells, in human DN (Figures 2A–C). Immunofluorescence staining showed marked Cf48 protein expression in tubular epithelial cells in DN, IgA nephropathy (IgAN), and lupus nephritis (LN), with little to no expression in normal human kidneys or in minimal change disease (Figures 2D–I). Contrast to high percentage of Cf48-positive cells in tubulointerstitum, very low percentage of Cf48-positive cells in glomeruli was observed in human DN (Supplementary Figure S2), albeit no mRNA was detectable in glomerular compartment *in situ* hybridization (Figure 2C). A similar expression pattern in glomeruli could be seen in mouse STZ-induced DN in *Nos3*$^{-/-}$ mice (Supplementary Figure S3).

The pattern of Cf48 expression was compared to markers of the thick ascending limb (Umod, NKCC2), proximal tubules (Lotus tetragonolobus lectin, LTL) and damaged/dedifferentiated tubules (VCAM1) (17-19). In normal human and mouse kidney, Cf48 is primarily expressed in the thick ascending limb as shown by co-localisation with Umod and NKCC2, and is largely absent from LTL+ proximal tubules (Supplementary Figures S4 and S5). In human DN, Cf48 expression is evident in the thick ascending limb, but is also seen in VCAM1+ dedifferentiated tubules, with Cf48 staining also seen in some dilated proximal tubules cells that weakly expressed LTL (Supplementary Figure S4). Similarly, in mouse CKD models, Cf48 expression is still seen in the thick ascending limb cells, but the main increase in Cf48 expression is evident in VCAM1+ dedifferentiated tubular cells, with little Cf48

expression seen in healthy looking proximal tubular cells with strong luminal LTL staining (Supplementary Figures S5-7).

Serum Cf48 levels correlate with loss of renal function in human CKD and as a potential biomarker of active fibrogenesis in a mouse model of CKD

Given the prediction of Cf48 as a secreted micropeptide (Supplementary Figures S1B and C), we examined serum Cf48 levels in patients with CKD. Low levels of Cf48 were detected in the serum of healthy controls (median 0.6750 ng/ml, IQR: 0.1463, 1.6760) and DM groups (median 1.3420 ng/ml, IQR: 0.7780, 2.1640). A 7 to 10-fold increase in Cf48 serum levels were evident in the DN, IgAN, and LN groups (Figure 2J, Supplementary Table S4). Analysis of the combined DN, LN and IgAN groups showed a negative correlation between serum Cf48 levels and renal function (eGFR), and a positive correlation with CKD stage (Figures 2K and L). This significant correlation between serum Cf48 levels and eGFR remained after multivariate analysis to adjust for potential confounding factors such as age, sex, and comorbidities (Supplementary Table S5). Further analysis was performed in each disease group. In DN patients (n=33), serum Cf48 levels correlated with reduced renal function (eGFR, serum creatinine and blood urea nitrogen levels) and CKD stage, but no correlation was evident with fasting blood glucose, hemoglobin A1C, 24-h urinary protein excretion or serum uric acid levels (Figures 3A-E). In the DN group, serum Cf48 levels also correlated with the pathological grade of disease and with the area of interstitial ACTA2 staining (myofibroblast accumulation, indicating active fibrosis)

(Figures 3F-H). In the LN group (n=20), serum Cf48 levels correlated with loss of renal function (eGFR, serum creatinine and BUN) and with CKD stage and pathological grade (Figures 3I-M). In the IgAN group (n=20), serum Cf48 levels correlated only with the pathological grade of disease (Supplementary Figure S8). Independent confirmation of our results was obtained from CKD studies in the NephroSeq database (20, 21). Increased Cf48 RNA levels in the tubulointerstitium correlated with a reduction in GFR in a European multicenter study and in a North American study (Supplementary Figures S9 and S10) (20, 21). In sum, these data suggest that Cf48 levels in both kidney and serum are associated with CKD stage.

To further clarify the relationship between serum Cf48 levels, renal function, and fibrosis, we have performed a sham or 15-min renal bilateral ischemia operation in C57BL/6J mice, a model of resolving acute renal failure. No difference in serum creatinine levels were evident on day 28 between IRI and sham groups – indicating recovery of renal function after IRI. However, mice that underwent IRI displayed marked renal fibrosis compared to the sham controls with a significant increase in staining for fibronectin, collagen IV, and Acta2+ myofibroblasts. Notably, serum Cf48 levels were substantially increased in the IRI group but not in the sham group (Supplementary Figure S11). Our data provide evidence that increase Cf48 levels are associated with renal fibrosis and are not dependent on renal function, and that serum Cf48 levels may be a potential biomarker of active fibrogenesis.

Cf48 overexpression enhances renal fibrosis in mouse CKD models

Transgenic (Tg) mice were created in which the *Cf48* open reading frame was driven by the CAG promoter in all cells following doxycycline treatment. Wild type (WT) and *Cf48-Tg* (Tg) mice given saline injections (controls) showed normal kidney function (serum cystatin C levels), urinary albumin excretion and kidney histology (Figures 4A-D); control Tg mice showed higher levels of kidney *Cf48* mRNA compared to control WT mice. Following induction of diabetes, *Cf48* mRNA levels were increased in both WT and Tg mice, although Cf48 expression was higher in Tg-DN compared to WT-DN mice (Supplementary Figure S12A). Type 1 diabetes was induced by low dose streptozotocin (STZ) injections, with an equivalent increase in fasting blood glucose levels and plasma HbA1c levels evident in WT and Tg mice (Supplementary Figures S12B and C). Tg-DN mice showed enhanced albuminuria and elevated serum cystatin C levels compared to WT-DN mice (Figures 4A-C). PAS staining showed glomerular matrix expansion and basement membrane thickening in some tubules in WT-DN mice, both of which were more prominent in Tg-DN (Figure 4D). Immunofluorescence staining showed increased collagen IV deposition in the glomerulus and tubulointerstitium of Tg-DN mice compared to WT-DN mice (Supplementary Figures S12D-E). A greater increase in fibronectin deposition and interstitial accumulation of Acta2 + myofibroblasts was also evident in Tg-DN versus WT-DN mice (Supplementary Figures S12D, F and G). Inflammation was enhanced in Tg-DN versus WT-DN mice based on monocyte chemoattractant protein-1

(*Mcp1/Ccl2*) and tumor necrosis factor (*Tnf*) mRNA levels, and infiltration of F4/80+ macrophages (Figures 4E-G).

We also investigated folic acid-induced nephropathy (FAN) in Tg mice, as a model of AKI-CKD transition (22). Acute renal failure (increased serum cystatin C levels) was not different between WT and Tg mice at day 2 FAN, indicating that Cf48 overexpression did not affect AKI in this model (Figure 4H). While renal function partially recovered by day 28 FAN in WT mice, renal function was significantly worse in Tg versus WT mice on day 28 FA based on serum cystatin C, serum creatinine and BUN levels (Figures 4I–K). Masson trichrome staining showed substantial renal interstitial fibrosis on day 28 FAN in WT mice, which was significantly increased in Tg mice (Figures 4L and M). Immunofluorescence staining showed a significant increase in the deposition of collagen IV and fibronectin and increased accumulation of Acta2 + myofibroblasts in day 28 FAN Tg mice compared to day 28 FAN WT mice (Supplementary Figure S12H-K). Day 28 FAN Tg mice also showed enhanced mRNA levels of proinflammatory cytokines (*Tnf*, *Il1b*, and *Ccl2*), increased mRNA levels of tubular epithelial cell injury markers (*Havcr1* and *Lcn2*), and infiltration of F4/80+ macrophages (Figures 4N-S). In sum, data from the DN and FAN models demonstrate that Cf48 overexpression enhanced renal fibrosis and inflammation in mouse CKD.

Cf48 deletion suppresses renal fibrosis in mouse CKD models

Given that overexpression of Cf48 enhances renal fibrosis, we sought to determine whether *Cf48* gene deletion would protect against fibrosis. Mice deficient in the *Cf48* open reading frame (*Cf48* KO) were generated. *Cf48* KO mice are healthy and viable, with no obvious abnormalities except for male homozygous *Cf48* KO mice being infertile. WT and *Cf48* KO mice were compared in the FAN model, with buffer injected mice serving as controls. Control KO mice had no detectable *Cf48* mRNA in the kidney (Figure 5A), and both control WT and KO mice showed normal renal function and structure (Figures 5B-G). Acute renal failure (increased serum cystatin C levels) was not different between WT and KO mice at day 2 FAN (Figure 5B). WT mice showed increased kidney *Cf48* mRNA and protein levels on day 28 FAN; however, no Cf48 mRNA or protein was detected in KO kidneys on day 28 FAN (Figure 5A**,** Supplementary Figure S13A). *Cf48* KO mice showed improved renal function on day 28 FAN compared to WT mice based on serum cystatin C, creatinine and BUN levels (Figures 5C-E). A significant reduction in renal fibrosis in KO versus WT mice on day 28 FAN was evident based on Masson trichrome staining, Western blotting for collagen I and Acta2, and immunofluorescence staining for collagen IV, Acta2 and fibronectin (Figures 5F–I, Supplementary Figures S13B-E). In addition, a significant reduction in renal inflammation was seen in KO versus WT mice on day 28 FAN based upon reduced kidney mRNA levels of *Il1b* and *Ccl2* (Figures 5J and K), and reduced infiltration of F4/80+ macrophages (Figure 5L).

Next, we tested *Cf48* KO mice in a surgically induced model of unilateral ureteral obstruction (UUO) in which mechanical pressure induces aggressive renal fibrosis (23). Masson trichome, immunohistochemistry, and confocal microscopy demonstrated that Cf48 deficiency decreased renal tubulointerstitial fibrosis and inflammation (Figures 5M and N, Supplementary Figures S13F-I). A substantial reduction in the F4/80+ macrophage infiltration was also evident in KO mice at day 7 UUO (Figures 5O and P). Thus, genetic approaches to overexpress or delete Cf48 establish that Cf48 regulates renal fibrosis and inflammation in three mouse CKD models of different etiologies.

Antisense Cf48 oligonucleotide treatment reduces renal fibrosis in mouse CKD models

Antisense Cf48 locked nucleic acid (LNA) oligonucleotides were tested as a therapeutic strategy to reduce renal fibrosis. LNA refers to an RNA oligonucleotide that has been modified to create an additional bridge connecting the 2' oxygen and the 4' carbon of the ribose ring, making it resistant to enzymatic degradation and improving its specificity and affinity as an oligonucleotide *in vivo* (24). Additionally, LNA oligonucleotides are preferentially taken up by the kidney after administration (25). First, we tested 2 different Cf48 LNAs in the UUO model. Mice received intraperitoneal injections of Cf48 LNA1, Cf48 LNA2, Cf48 LNA1 + LNA2, or control LNA (CTL LNA) on days 1 and 4 after UUO with mice killed on day 7. Western blotting showed a strong upregulation of Cf48 protein levels in the CTL

LNA treated UUO compared to the sham surgery group (Figure 6A). As single treatments, Cf48 LNA1 and LNA2 gave only minor reductions in Cf48 protein expression; however, the combination of Cf48 LNA1 + LNA2 was highly effective in knocking down Cf48 expression (Figure 6A). Thus, subsequent experiments used Cf48 LNA1 + LNA2 (referred to as Cf48 LNA), which produced a substantial reduction in renal fibrosis as shown by Western blotting for collagen I and Acta2 (Figures 6B and C), and collagen deposition based on Masson trichrome staining (Figures 6D and E). In addition, Cf48 LNA treatment significantly reduced infiltration of F4/80+ macrophages (Figures 6F and G).

We tested Cf48 LNA treatment as an early intervention treatment in DN using the STZ-DN model in susceptible *Nos3*$^{-/-}$ mice. Diabetic *Nos3*$^{-/-}$ mice were treated with Cf48 LNA or CTL LNA given once weekly from week 3 until being killed at week 8. Treatment with Cf48 LNA did not affect fasting blood glucose or HbA1C levels (Figures 6H and I). However, Cf48 LNA treatment significantly decreased albuminuria and protected against loss of renal function (Figures 6J–L). Furthermore, Cf48 LNA treatment significantly reduced glomerular matrix expansion as indicated by PAS staining (Figure 6M), and confirmed by immunostaining (Figure 6N) and quantification of the area of glomerular collagen IV deposition (Figure 6O). Interstitial accumulation of Acta2 + myofibroblasts was also reduced by Cf48 LNA treatment (Figure 6N), in concert with a reduction in inflammation as indicated by *Ccl2* mRNA levels (Figure 6P). Collectively, these data demonstrate that Cf48 LNA

administration inhibits endogenous Cf48 expression in the kidney, reduces renal fibrosis in the aggressive UUO model, and retards the progression of established DKD.

Cf48 enhances the TGF-β1-induced fibrotic response via the transferrin receptor (TFRC)

Given that tubular epithelial cells are the main site of Cf48 expression in human and mouse kidney disease, we investigated whether factors implicated in development of CKD induced tubular Cf48 production. Stimulation of human tubular epithelial cells (HK2) with TGF-β1, TNF, angiotensin II or CoCl2 all increased expression of the Cf48 peptide (Supplementary Figure S14), suggested that profibrotic, proinflammatory, overactivated renin-angiotensin system and hypoxic conditions may induce expression of Cf48 in renal tubular epithelial cells.

While tubular cells are the main site of Cf48 production in the injured kidney, it is fibroblasts/myofibroblasts that are the main cell types responsible for pathogenic collagen deposition (26). Therefore, we hypothesized that Cf48 may enhance the fibrotic response in a paracrine fashion. We generated a recombinant form of the secreted Cf48 peptide (rCf48) which lacked the signal peptide (Figure 7A). The addition of rCf48 to NRK49F renal fibroblasts has no effect by itself but enhanced the TGF-β1 profibrotic response (Figures 7B and C). Similarly, addition of rCf48 to NRK52E tubular epithelial cells had no effect by itself, but enhanced TGF-β1-

induced dedifferentiation with increased expression of Acta2, collagen I, and fibronectin, and a reduction in Cadherin-1 expression (Figure 7D).

Smad3 is activated by C-terminal phosphorylation and plays an essential role in the TGF-β1-induced fibrotic response (27). The addition of rCf48 to NRK49F renal fibroblasts did not induce Smad3 phosphorylation or enhance TGF-β1 induced Smad3 phosphorylation (Figure 7E, top). In addition, rCf48 failed to induce Smad3 transcriptional activity or modify TGF-β1-induced Smad3 transcriptional activity (Figure 7E, bottom). Pathways involved in non-canonical TGF-β1 signaling were investigated; however, rCf48 did not induce phosphorylation of p38 Mapk, Erk1/2 or Jnk1/2 in renal fibroblasts, nor did Cf48 affect phosphorylation of these kinases in response to TGF-β1, TNF or Ang-II (Figure 7F, Supplementary Figure S15).

Next, we looked for evidence of rCf48-induced covalent modification of proteins in renal fibroblasts and proximal tubular epithelial cells 30 min after rCf48 addition. However, a Western blot-based screen using antibodies to detect phosphotyrosine, acetyllysine, propionyllysine, butyryllysine, succinyllysine, crotonyllysine, 2-hydroxyisobutyryllysine, malonyllysine, ubiquitin, sumo1/2/3, glutaryllysine, β-hydroxybutyryllysine, and lactyllysine modifications revealed no obvious changes (data not shown). As this appeared to rule out conventional receptor-based signaling pathways, we investigated whether the rCf48 peptide is endocytosed into cells in order to exert its effects without protein modification. To address this possibility,

NRK49F cells were incubated with varying concentrations of flag-tagged rCf48 for different periods of time. Western blotting detected flag-rCf48 uptake in NRK49F cells after 30 min, which peaked at 2–4 h, and uptake of flag-rCf48 increased as the amount of flag-rCf48 added to cells was increased (Figure 7G). Confocal imaging showed a perinuclear distribution of flag-rCf48 uptake in NRK49F cells at 2 h (Figure 7H). To examine Cf48 uptake by cells in the fibrosing kidney, day 14 FAN mice were given flag-rCf48 by tail vein injection and then killed 5 min later. Confocal imaging revealed flag-rCf48 uptake by Acta2 + myofibroblasts *in vivo* (Figure 7I). These data suggest that Cf48 produced by tubular cells can act on fibroblasts in a paracrine fashion, although the mechanism of uptake into fibroblasts is unclear.

We investigated potential Cf48 binding proteins in 293T cells using immunoprecipitation couple to mass spectroscopy (IP/MS) which identified the transferrin receptor (TFRC/CD71) as a potential Cf48 receptor (Supplementary Table S6). TFRC is a cell surface receptor that uptakes iron into the cell via receptor-mediated endocytosis and is a receptor for new-world arenaviruses (28, 29). Confocal microscopy demonstrated that Tfrc is expressed in renal tubular epithelial cells and Acta2 + myofibroblasts (Figure 7J). IP/MS and surface plasmon resonance studies confirmed the interaction between Cf48 and TFRC (Figures 7K and L). Use of a neutralizing anti-Tfrc antibody or siRNA-mediated Tfrc knockdown significantly reduced rCf48 uptake by NRK49F renal fibroblasts (Figures 7M and N). Furthermore, Tfrc knockdown in NRK49F renal fibroblasts abrogated rCf48 enhancement of TGF-

β1-induced *Acta2, Serpine1* and *Ccn2* mRNA expression (Figure 7O). These data identify Tfrc as the main receptor through which Cf48 enhances the TGF-β1-induced fibrotic response.

Quantitative proteomic analysis identifies downregulation of extracellular matrix products in FA nephropathy in Cf48 deficient mice

To investigate molecular mechanism(s) by which Cf48 promotes renal fibrosis, MS-based quantitative proteomic analysis of kidney samples from Cf48-deficient and WT mice on day 28 after FA or vehicle administration was performed and identified 8,286 quantifiable proteins in the four experimental groups with three biological replicates using 4D-DIA proteomic quantification. We defined significantly different ($P < 0.05$ by two-tailed t-test) proteins and used a criterion of ≥ 1.5-fold change between two groups as differential protein candidates. Subsequently, the numbers of downregulated and upregulated proteins in the four groups were identified (Supplementary Table S7). Cluster of orthologous groups (COG) classification analysis revealed molecules in the category of translation, and ribosomal structure and biogenesis were upregulated in FAN KO group compared with the FAN WT group, while molecules classified in the categories of nucleotide transport and metabolism, RNA processing and modification, posttranslational modification, protein turnover, chaperones, and extracellular structures were downregulated (Supplementary Table S8). This indicated a selective effect of Cf48 deficiency on certain COGs. As one example, Serpine1 protein levels were reduced by > 50% in the FAN KO group

compared to the FAN WT group (Figure 8A). A separate analysis of kidney samples confirmed that Cf48 deficiency decreased Serpine1 production at the mRNA and protein levels in the FAN model (Figures 8B and C). A retroviral vector was used to express a green fluorescent protein (GFP), with or without full-length Cf48, in renal fibroblasts. Western blots of GFP-expressing cells showed that Cf48 overexpression enhanced TGF-β1-induced upregulation of Serpine1, Acta2 and collagen I proteins (Figure 8D). We investigated cobalt chloride (CoCl2) induced hypoxia-inducible factors as a second stimulus to induce Serpine1 expression. Use of viral-induced Cf48 overexpression, or the addition of rCf48 peptide, did not affect basal *Serpine1* mRNA levels in renal fibroblasts; but this did significantly increase CoCl2-induced upregulation of *Serpine1* mRNA (Figures 8E and F). Given the importance of Serpine1 in renal fibrosis (30), we investigated how Cf48 regulates Serpine1 expression in renal fibroblasts.

Cf48 is a mRNA-binding peptide that interacts with and stabilizes Serpine1 mRNA

Cf48 increased Serpine1 production at mRNA and protein levels in renal fibroblasts. In addition, Cf48 interacts with SERBP1 (Supplementary Table S6), a mRNA-binding protein that binds to the 3'-most 134 nucleotides of *Serpine1* mRNA and acts to destabilize *Serpine1* mRNA (31). Using an RNA Electrophoretic Mobility Shift Assay (RNA-EMSA), we demonstrated that Cf48 can bind to 3'-most 134 nucleotides of *Serpine1* mRNA. Mutation at SERBP1 binding site 1, but not at binding site 2,

abolished the interaction between rCf48 and *Serpine1* mRNA (Figures 8G and H), indicating that Cf48 is a mRNA-binding peptide. Renal fibroblasts were stimulated with TGF-β1 for 6 h to increase *Serpine1* mRNA levels, then actinomycin D was added to stop transcription and enable mRNA decay assessment by RT-qPCR in the presence or absence of Cf48. rCf48 increased the half-life of *Serpine1* mRNA from an estimated 2.06 h to 5.27 h and the half-life of *Acta2* mRNA from 3.14 h to 6.16 h (Figure 8I, Supplementary Figure S16). WB and an enzyme activity assay demonstrated Cf48 enhanced TGF-β1-induced upregulation of Serpine1 protein level and activity after actinomycin D treatment in renal fibroblasts (Supplementary Figure S17). RNA immunoprecipitation-sequencing (RIP-seq) was performed for a broader view of Cf48 as a mRNA-binding protein. This found that Cf48 can bind to various RNAs (Supplementary Table S9), identifying 1515 Cf48 target RNAs, including *Acta2*, *Serpine1, Ccn2* and *Col4a1* (Supplementary Table S10, Figure 8J). GO & KEGG analysis further revealed extracellular matrix structural constituent is one of the major Cf48 binding mRNAs (Supplementary Table S11). We also corroborated rCf48 binding to 3'-most 132 nucleotides of the *Acta2* mRNA via RNA-EMSA (Figures 8K and L). Vimentin (Vim) was not identified as a Cf48 target, and therefore served as a negative control in RNA-EMSA studies with no interaction between rCf48 and the *Vim* mRNA probe seen (data not shown), even though it contains the proposed rCf48 binding consensus "AAAAAA". These data suggest that other factors may be required for the interaction between the Cf48 peptide and the targeted RNA, which warrants further investigation.

To corroborate the proposed mechanism identified in animals, primary human renal fibroblasts were employed. The addition of Cf48 to human renal fibroblasts enhanced TGF-β1-induced production of ACTA2, collagen I and SERPINE1 (Supplementary Figure S18A). Knockdown of TFRC by siRNA decreased uptake of Flag-Cf48 and almost abrogated Cf48 enhancement of the TGF-β1-induced fibrotic response (Supplementary Figures S18B-D). Furthermore, Cf48 increased the half-life of SERPINE1 mRNA (Supplementary Figure S18E). Taken together, our studies provided evidence that Cf48 promotes the TGF-β1-induced fibrotic response via the TFRC and an increase in the half-life of profibrotic gene mRNAs in both human and animal renal fibroblasts.

DISCUSSION

The present study identified Cf48 as a secreted micropeptide that is upregulated in both serum and kidneys across several types of human CKD (DN, LN and IgAN), and upregulated in the kidney across 3 mouse CKD models. Serum Cf48 levels are strongly associated with loss of renal function in human DN. Overexpression, knockout, or knockdown of Cf48 modulates renal fibrosis across 3 pathologically distinct mouse CKD models. Mechanistic studies demonstrate that TFRC mediates the uptake of Cf48 into renal fibroblasts. Cf48 interacts with mRNAs of profibrotic molecules, including *Acta2*, *Collagen IV*, *Ccn2* and *Serpine1*, and stabilizes *Serpine1* mRNA. Our study provides robust evidence that Cf48 is a secreted peptide that enhances renal fibrosis and is a potential therapeutic target.

APOC1

Ribosome profiling and bioinformatics analysis identified four secreted peptides as candidates to have a profibrotic function in mouse DN, including Cf48, Apoc1, Hilpda, and Tmsb4x. While Cf48 was selected for further investigation, two of the other peptides have been implicated in renal fibrosis. Apolipoprotein C1 (Apoc1) is an inhibitor of lipoprotein binding to the low-density lipoprotein (LDL) receptor, LDL receptor-related protein, and very low-density lipoprotein receptor (32). Patients with DM have a higher APOC1 plasma level, and meta-analysis demonstrates an association between a polymorphism in *APOC1* and an increased risk of developing nephropathy (33). *Apoc1* Tg mice exhibited albuminuria, renal dysfunction,

glomerulosclerosis, inflammatory cell infiltration, and increased inflammatory cytokine and fibrotic growth factor expressions (34), suggesting that Apoc1 may play a role in DN pathogenesis. Thymosin beta 4 (Tmsb4x) is a peptide which acts to suppress renal fibrosis (35), and loss of endogenous Tmsb4x accelerates kidney disease (36). The identification of these peptides supports the effectiveness the screening strategy employed.

Cf48 in the brain and the male reproductive organs

Cf48 was first characterized by Endele et al. (37) as a putative evolutionarily conserved neuropeptide. It is one of the three genes within a DNA microdeletion found in a patient with a mild form of Wolf–Hirschhorn syndrome. Western blotting showed Cf48 protein expressed in brain tissue but absent in other organs. *In situ* hybridization and northern blotting demonstrated Cf48 expression in different zones during cortical and cerebellar development, and Cf48 expression in all cortical and subcortical regions of the adult mouse brain (37). The function of Cf48 was not studied although Cf48 was proposed to be involved in intellectual and fine motor disabilities based on its pattern of expression. Very recently, Cf48 (NICOL1) was identified as a secreted protein expressed in mouse male reproductive organs. Cf48 plays an important role in lumicrine-mediated sperm maturation and male fertility through interaction with NELL2 (38). Male homozygote Cf48 knockout mice are infertile (38). Our study confirmed that male homozygote Cf48 knockout mice are infertile, and that Cf48 is expressed at very low levels in normal adult kidneys.

However, Cf48 was upregulated in both human and mouse CKD. We also demonstrated that the secreted form of Cf48 enhances the TGF-β1-induced fibrotic response. In addition, our IP/Mass spectrometry study in 293T cells did not identify the interaction between Cf48 and NELL2 (Supplementary Table S6). Thus, it may be that Cf48 plays distinct roles in different organs.

Do serum Cf48 levels predict progression of CKD?

Serum Cf48 peptide levels correlated with loss of kidney function, disease stage and pathological grade of disease in human CKD. Indeed, renal interstitial fibrosis is a strong predictor of the progression of CKD to ESRD (4-6). However, renal fibrosis is a stochastic process with biopsies showing varying degrees of active and inactive fibrosis, with active fibrotic lesions identified by the presence of ACTA2 + myofibroblasts. The finding that serum Cf48 peptide levels correlated with the area of ACTA2 + myofibroblast staining in renal biopsies, and that serum Cf48 levels were significantly increased while serum levels of creatinine reduced to a normal range in a mouse model of resolving AKI accompanying renal fibrosis, indicates that serum Cf48 could be a biomarker of active renal fibrosis, and potentially predictive of disease progression. However, our study could not rule out the possibility that the correlation between higher plasma Cf48 levels and reduced eGFR could be due to reduced glomerular filtration of the circulating Cf48 peptide .

Another limitation of our current study is that it uses a cross-sectional design at a single time point. To move these findings towards the clinic, our group is currently undertaking prospective studies in larger patient cohorts to define the range of serum Cf48 levels that are associated with active renal fibrosis, and to determine whether serum Cf48 levels can predict the loss of renal function over time.

TFRC mediates uptake of Cf48 into renal tubular epithelial cells and fibroblasts

TFRC can bind and uptake multiple ligands into the cell. While best known for the cellular uptake of iron through endocytosis (28), TFRC is a receptor for new-world hemorrhagic fever arenaviruses (29), and can endocytose IgA (39). The affinity (KD) between TFRC and Cf48 is 5.71×10^{-7} M, indicating that it is not a strong interaction and Cf48 may be easily released from TFRC after endocytosis. Antibody-based blockade or siRNA-mediated knockdown of TFRC was effective in preventing Cf48 uptake and function in renal fibroblasts. Supporting a role for TFRC in renal fibrosis are studies in which mice heterozygous for the *Tfrc* gene show reduced renal fibrosis in the UUO and DN models (40). However, how Cf48 interacts with TFRC remains to be investigated. Finally, it remains to be determined whether Cf48 can bind to other cell-surface receptors in kidneys.

Cf48 is a potential antifibrotic target independent of TGF-β/Smad3 signaling

TGF-β/Smad signaling plays a central role in fibrogenesis (41). However, TGF-β1 is a multifunctional protein involved in various processes, including cell differentiation,

and is a negative regulator of the immune system. Indeed, complete TGF-β1 blockade causes uncontrolled immune-mediated organ destruction in neonatal mice (42). A key feature of the Cf48 peptide is that it enhances renal fibrosis without activating, or altering the TGF-β/Smad signaling pathway. Thus, targeting endogenous Cf48 expression and/or function may circumvent the concerns associated inhibiting the TGF-β/Smad signaling pathway itself. Supporting Cf48 as a potential therapeutic target, mice lacking *Cf48* are healthy and protected from renal fibrosis. Our study provides new therapeutic opportunities to target renal fibrosis. Cf48 expression may be inhibited via a siRNA or LNA-based oligonucleotide approach, while the function of the extracellular Cf48 peptide could be targeted by a neutralizing antibody. It may also be possible to design a TFRC antagonist that can prevent Cf48 binding, and thus Cf48 profibrotic action, without affecting transferrin uptake. Finally, further dissection of the mechanism of action of the Cf48 peptide may unveil a new paradigm in the regulation of the fibrotic response.

Our *in vitro* and *in vivo* studies provide evidence that Cf48 enhances renal fibrosis. However, renal fibrosis and inflammation are tightly linked in the pathogenesis of CKD, and effects of Cf48 on inflammation (cytokine expression and macrophage infiltration) were evident. Thus, a role for Cf48 in promoting inflammation may contribute to the overall pro-fibrotic effect of Cf48 in the development and progression of CKD. Dissecting the contribution of Cf48 to inflammation *per se* warrants further investigation.

Cf48 is an RNA binding protein (RBP)

RBPs interact with various RNAs to play fundamental roles in post-transcriptional and translational processes (43). Dysfunctional RBPs are associated with human diseases, such as genetic disorders (44) and cancer (45). Far upstream element-binding protein 1 (FUBP1) binds to the 3'UTR of polycystic kidney disease 2 (PKD2) mRNA to inhibit PKD2 translation (46). RIP-seq reveals that Cf48 interacts with extracellular matrix structural constituent mRNAs, including *Serpine1, Acta2, Ccn2* and *Col4a1*. RNA-EMSA confirmed rCf48 binding to *Serpine1* and *Acta2* mRNA consensus "AAAAAA" sequence, while an RNA decay study showed that Cf48 increased the half-life of *Serpine1* mRNA. The direct binding of SERBP1 to the 3'-most 134 nucleotides of the *Serpine1* mRNA increases its degradation (31). Cf48 may compete with SERBP1 to bind to *Serpine1* mRNA, thus avoiding mRNA degradation, enhancing mRNA accumulation and protein production which promotes fibrosis. The proposed rCf48 binding mRNA consensus "AAAAAA" is not a relatively specific binding site. We also identified potential Cf48 binding proteins in 293T cells using immunoprecipitation couple to mass spectroscopy (IP/MS) (Supplementary Table S6). This could involve other protein(s) that are required to enable effective binding of the Cf48 peptide to the specific target mRNAs; however, investigation of such a possibility will be the subject of a new study.

Tubulopathy vs glomerulopathy

Renal tubular epithelial cells have a very high demand for energy to fulfill their extensive reabsorption and secretion functions, making these cells susceptible to diverse insults such as hypoxia, hypertension, hyperglycemia, proteinuria, toxins, and mechanical stress. Tubular epithelial cells may undergo dedifferentiation after injury, developing a profibrotic and proinflammatory phenotype that drives CKD progression (47). Our study revealed that Cf48 is predominantly expressed in renal tubular epithelial cells in CKD, and Cf48 promoted dedifferentiation in cultured proximal tubular epithelial cells. Cf48 overexpression or deletion/knockdown modulated renal interstitial fibrosis and CKD progression. Thus, while the Cf48 micropeptide clearly affects tubular epithelial cells and fibroblasts in the tubulointerstitial compartment of the kidney, the role of Cf48 in glomerular damage is much less clear. Of note, *Cf48* Tg mice showed enhanced glomerular collagen deposition in the STZ-DN model, and Cf48 LNA treatment reduced glomerular collagen deposition in the *Nos3*$^{-/-}$ STZ-DN model. Thus, despite there being few Cf48-positive cells in the glomerular compartment, Cf48 still modified glomerulosclerosis. The impact of Cf48 on glomerular cells may be via direct interaction with mRNAs to promote fibrosis and/or inflammation, or via indirect actions through increased circulating levels of profibrotic and/or proinflammatory cues, such as Ccn2. Indeed, TRFC is upregulated in glomerular mesangial cells in patients with progressive IgAN and Henoch-Schonlein Purpura (48, 49), although little information on podocyte TRFC expression is available. As the study used whole body overexpression or knockout of Cf48 in mice, the specific role of tubular cell production of Cf48 was not addressed, nor was

the question of whether tubular cell derived Cf48 acts in a paracrine fashion on renal interstitial fibroblasts and glomerular cells. The systemic effect could not be ruled out. Thus, an important area for future investigation is to determine how tubular cell-derived Cf48 acts to promote glomerulosclerosis and tubulointerstitial fibrosis in CKD.

In summary, our study identifies Cf48 as a micropeptide that enhances renal fibrosis independent of the TGF-β/Smad signaling pathway. A strong correlation was seen between serum Cf48 levels and loss of renal function. TFRC was identified as a Cf48 receptor, and Cf48 was shown to act as an RBP to regulate RNA metabolism and gene expression. These findings identify serum Cf48 levels as a potential biomarker of active renal fibrosis, while pharmacological approaches to inhibit Cf48 expression, neutralize the Cf48 peptide, or target the Cf48 peptide receptor, represent therapeutic opportunities for the treatment of CKD.

MATERIALS AND METHODS

Sex as a biological variable

Serum and biopsy samples were obtained from both males and females for analysis of Cf48 expression, with similar findings seen in both sexes. Female mice are resistant to streptozotocin-induced diabetes, and so this model was performed only in male mice. Both the UUO model (50) and the FA model (51) are induced equally in male and female mice; therefore, we performed studies in only male mice in order to minimize animal use (recognizing the goal of animal ethics for replacement, reduction and refinement), knowing that the results are highly likely to apply equally to both sexes.

Study design

The objective of the study was to investigate the role of the C4orf48 (Cf48) micropeptide in CKD. Serum levels of the Cf48 peptide were measured by ELISA (CSB-EL003989HU, CUSABIO, China) in a cohort of patients with CKD (DN, IgAN, LN) undergoing renal biopsy in the Department of Nephrology, the First Affiliated Hospital of Sun Yat-Sen University from June 2020 to December 2021 (see Supplementary Table S4). Controls included diabetic individuals without kidney disease and healthy controls (serum only). Serum Cf48 levels were compared between groups and correlated with kidney function and features of kidney biopsies. Indirect immunofluorescence staining for Cf48 was performed in formalin-fixed paraffin sections of renal biopsies using rabbit monoclonal anti-Cf48 antibody (ab185315, Abcam, UK).

Transgenic mice with doxycycline-inducible ubiquitous expression of *C4orf48* (gm1673) under the CAG promoter, and *Cf48* knockout mice, were created by Cyagen Biosciences (Supplementary Figure S19 and 20, Guangzhou, China). Homozygote *Cf48* knockout and wild type mice were produced by crossbreeding of heterozygous mice. Male homozygote *Cf48* knockout mice were infertile, which is consistent with the report by Kiyozumi et al (38). *Nos3*$^{-/-}$ mice were obtained from Jackson Labs (strain 002684). All mouse lines were on the C57BL/6J background and bred at Sun Yat-Sen University Animal Services and Guangdong Medical University Animal Services. Age- and sex-matched littermates were used as wild-type (WT) controls.

Mice were used in 3 contrasting models of CKD. Diabetic nephropathy (DN) was induced in 8-week-old mice by low-dose streptozotocin (STZ, Sigma-Aldrich, USA, 55 mg/kg) in 0.1 mmol/L sodium citrate buffer (pH 4.5) given intraperitoneally once daily for 5 days (16). Folic acid nephropathy (FAN) was induced 8-week-old mice by intraperitoneal injection of 250 mg/kg folic acid (Sigma-Aldrich, USA) in 0.3 mol/L sodium bicarbonate, with AKI assessed by renal function on day 2 and CKD assessed on day 28 (22). Renal interstitial fibrosis was induced by unilateral ureteral obstruction (UUO) surgery as previously described (23). Measurement of kidney function, blood glucose levels, kidney histology, kidney immunostaining, RNA analysis, and Western blotting are described in the Supplementary Methods.

Mouse Cf48 LNA and control LNA were designed by and purchased from QIAGEN (Hilden, Germany). LNA sequences are shown in Supplementary Methods. In the UUO model, LNAs were administered by intraperitoneal injection on days 1 and 4 after surgery and then animals were killed on day 7. In the STZ-DN model induced in *Nos3*$^{-/-}$ mice, LNAs were administered by weekly injection on weeks 3 to 8 after STZ administration and then animals were killed.

The ability of recombinant Cf48 peptide to enhance the fibrotic response of normal rat kidney fibroblasts (NRK49F cells, CRL-1570, ATCC, USA) or normal rat kidney epithelial cells (NKR52E cells, CRL-1571, ATCC, USA) was tested in the presence and absence of TGF-β1. Recombinant Flag-tagged mouse Cf48 peptide (see Supplementary Table S12) was purified from Chinese Hamster Ovary cells and used in studies of peptide uptake by renal fibroblasts and tubular cells *in vitro* and *in vivo*. Immunoprecipitation couple to mass spectroscopy identified the transferrin receptor (TFRC/CD71) as a potential Cf48 receptor. Use of a neutralizing Tfrc antibody or Tfrc siRNA blocked Cf48 peptide uptake and biological response in NRK49F cells.

Kidney tissues from *Cf48* knockout and WT mice on day 28 FAN were analysed by mass spectrometry-based 4D-DIA proteomic quantification and Cluster of Orthologous Groups classification which showed downregulation of extracellular matrix products in *Cf48* knockout mice. The role of Cf48 as an RNA binding peptide

for mRNAs species involved in the fibrotic response was investigated by RNA immunoprecipitation-sequencing, RNA Electrophoretic Mobility Shift Assay, and RNA decay studies.

Statistical analysis.

Data are presented as mean ± SD. Statistical comparisons between two groups were conducted using the 2-tailed Student's t-test, or by 1-way analysis of variance (ANOVA) followed by Tukey's multiple comparison test for 3 or more groups. Correlation analysis of parametric data without normal distribution used Spearman's coefficient. A P value less than 0.05 was considered significant. Analyses were performed using GraphPad Prism version 8.0 (GraphPad Software, San Diego, CA) and SPSS 24.0 Software.

Study approval

The human study was reviewed and approved by the First Affiliated Hospital of Sun Yat-Sen University Institutional Review Boards (IRB approved number [2016] 215, Guangzhou, China). All patients gave their written informed consent. All animal studies were reviewed and approved by the Sun Yat-Sen University Institutional Animal Care and Use Committee (No. SYSU-IACUC-2022-000134, -000361, -000943) and the Guangdong Medical University Institutional Animal Care and Use Committee (No. GDY2204005).

Supplementary Materials

Supplementary Figures

Supplementary Figure S1. Cf48 is a highly conserved and secreted micropeptide.

Supplementary Figure S2. Cf48 expression in human kidneys.

Supplementary Figure S3. Cf48 expression in mouse kidneys.

Supplementary Figure S4. Expression of Cf48 in normal control and human diabetic nephropathy.

Supplementary Figure S5. Expression of Cf48 in normal control and 3 mouse models of renal fibrosis.

Supplementary Figure S6. Expression of Cf48 and Vcam1 in normal control and 3 mouse models of renal fibrosis.

Supplementary Figure S7. Expression of Cf48, Nkcc2 and Umod in normal control and 3 mouse models of renal fibrosis.

Supplementary Figure S8. Correlations between clinical indices and serum Cf48 levels in human IgAN.

Supplementary Figure S9. *Cf48* mRNA levels in the kidney tubulointerstitium correlate with renal function in chronic kidney disease.

Supplementary Figure S10. Kidney *Cf48* mRNA levels correlate with renal function in chronic kidney disease.

Supplementary Figure S11. Serum Cf48 levels are increased in mice with developing renal fibrosis following ischemia reperfusion injury (IRI).

Supplementary Figure S12. Overexpression of Cf48 promotes renal fibrosis in mouse models of CKD.

Supplementary Figure S13. Cf48 deficiency suppressed renal fibrosis in mouse models of CKD.

Supplementary Figure S14. Induction of Cf48 expression under various conditions in HK2 cells.

Supplementary Figure S15. Effect of rCf48 on the p38 Mapk, Erk1/2 and Jnk1/2 signaling pathways in NKR49F cells.

Supplementary Figure S16. Cf48 increased the half-life of *Acta2* mRNA.

Supplementary Figure S17. Cf48 enhanced TGF-β1-induced upregulation of *Serpine1* protein and activity in renal fibroblasts.

Supplementary Figure S18. Cf48 enhanced the TGF-β1-induced fibrotic response in primary human renal fibroblasts.

Supplementary Figure S19. Schematic diagram outlining the construct used for generating the *C4orf48* transgenic mouse line.

Supplementary Figure S20. Generation of the *C4orf48* gene knockout mouse line.

Supplementary Table S1. Control (age-matched *Nos3*$^{-/-}$) vs *Nos3*$^{-/-}$ DN gene annotation (Ribo-seq).

Supplementary Table S2. Control (age-matched *Nos3*$^{-/-}$) vs *Nos3*$^{-/-}$ DN gene filter annotation (Ribo-seq).

Supplementary Table S3. Control (age-matched *Nos3*$^{-/-}$) vs *Nos3*$^{-/-}$ DN gene ontology enrichment analysis (Ribo-seq): Cellular Components.

Supplementary Table S4. Characteristics of CKD patients among groups.

Supplementary Table S5. Multiple linear regression analysis of the risk factors for eGFR in CKD patients.

Supplementary Table S6. IP/MS identified Cf48 interacting proteins.

Supplementary Table S7. Differentially expressed protein summary (Filtered with threshold value of expression fold change and two-tailed two-sample t-tests (p value < 0.05)).

Supplementary Table S8. Differentially expressed protein summary (KO_FA/WT_FA). (Filtered with threshold value of expression of 1.5 fold change and two-tailed two-sample t-tests p value < 0.05).

Supplementary Table S9. RIP-seq analysis reveals IP and Input RNA read counts.

Supplementary Table S10. RIP-seq analysis reveals Cf48 targets (RNAs).

Supplementary Table S11. Gene Ontology analysis reveals Cf48 Cellular Components.

Supplementary Table S12. Recombinant Fc-Flag-Cf48 protein sequence.

Supplementary Table S13. cDNA primers used in real-time PCR measurements.

Supplementary Table S14. Rat Tfrc and human TFRC siRNA and NC siRNA sequences

Supplementary Materials and Methods.

REFERENCES

1. Ruiz-Ortega M, et al. Targeting the progression of chronic kidney disease. *Nat Rev Nephrol.* 2020;16(5):269-288.
2. Chen TK, et al. Chronic Kidney Disease Diagnosis and Management: A Review. *JAMA.* 2019;322(13):1294-1304.
3. Heerspink HJL, et al. Renoprotective effects of sodium-glucose cotransporter-2 inhibitors. *Kidney Int.* 2018;94(1):26-39.
4. Risdon RA, et al. Relationship between renal function and histological changes found in renal-biopsy specimens from patients with persistent glomerular nephritis. *Lancet.* 1968;2(7564):363-366.
5. Nath KA. Tubulointerstitial changes as a major determinant in the progression of renal damage. *Am J Kidney Dis.* 1992;20(1):1-17.
6. Katz A, et al. An increase in the cell component of the cortical interstitium antedates interstitial fibrosis in type 1 diabetic patients. *Kidney Int.* 2002;61(6):2058-2066.
7. Waikar SS, et al. Relationship of proximal tubular injury to chronic kidney disease as assessed by urinary kidney injury molecule-1 in five cohort studies. *Nephrol Dial Transplant.* 2016;31(9):1460-1470.
8. Zeni L, et al. A more tubulocentric view of diabetic kidney disease. *J Nephrol.* 2017;30(6):701-717.
9. Gilbert RE. Proximal Tubulopathy: Prime Mover and Key Therapeutic Target in Diabetic Kidney Disease. *Diabetes.* 2017;66(4):791-800.
10. Yang L, et al. Epithelial cell cycle arrest in G2/M mediates kidney fibrosis after injury. *Nat Med.* 2010;16(5):535-543.
11. Kondo T, et al. Small peptide regulators of actin-based cell morphogenesis encoded by a polycistronic mRNA. *Nat Cell Biol.* 2007;9(6):660-665.
12. Slavoff SA, et al. A human short open reading frame (sORF)-encoded polypeptide that stimulates DNA end joining. *J Biol Chem.* 2014;289(16):10950-10957.

13. Lee C, et al. The mitochondrial-derived peptide MOTS-c promotes m etabolic homeostasis and reduces obesity and insulin resistance. *Cell Metab.* 2015;21(3):443-454.
14. Matsumoto A, et al. mTORC1 and muscle regeneration are regulated by the LINC00961-encoded SPAR polypeptide. *Nature.* 2017;541(7636):228-232.
15. Guo B, et al. Humanin peptide suppresses apoptosis by interfering with Bax activation. *Nature.* 2003;423(6938):456-461.
16. Nakagawa T, et al. Diabetic endothelial nitric oxide synthase knockout mice develop advanced diabetic nephropathy. *J Am Soc Nephrol.* 2007;18(2):539-550.
17. Kirita Y, et al. Cell profiling of mouse acute kidney injury reveals conserved cellular responses to injury. *Proc Natl Acad Sci U S A.* 2020;117(27):15874-15883.
18. Ide S, et al. Ferroptotic stress promotes the accumulation of pro-inflammatory proximal tubular cells in maladaptive renal repair. *Elife.* 2021;10:e68603.
19. Gerhardt LMS, et al. Single-nuclear transcriptomics reveals diversity of proximal tubule cell states in a dynamic response to acute kidney injury. *Proc Natl Acad Sci U S A.* 2021;118(27):e2026684118.
20. Martini S, et al. Integrative biology identifies shared transcriptional networks in CKD. *J Am Soc Nephrol.* 2014;25(11):2559-2572.
21. Sampson MG, et al. Integrative Genomics Identifies Novel Associations with APOL1 Risk Genotypes in Black NEPTUNE Subjects. *J Am Soc Nephrol.* 2016;27(3):814-823.
22. Jiang M, et al. Combined Blockade of Smad3 and JNK Pathways Ameliorates Progressive Fibrosis in Folic Acid Nephropathy. *Front Pharmacol.* 2019;10:880.
23. Qu X, et al. The Smad3/Smad4/CDK9 complex promotes renal fibrosis in mice with unilateral ureteral obstruction. *Kidney Int.* 2015;88(6):1323-1335.
24. Petersen M, and Wengel J. LNA: a versatile tool for therapeutics and genomics. *Trends Biotechnol.* 2003;21(2):74-81.

25. Broos K, et al. Particle-mediated Intravenous Delivery of Antigen mRNA Results in Strong Antigen-specific T-cell Responses Despite the Induction of Type I Interferon. *Mol Ther Nucleic Acids.* 2016;5(6):e326.

26. Kuppe C, et al. Decoding myofibroblast origins in human kidney fibrosis. *Nature.* 2021;589(7841):281-286.

27. Sato M, et al. Targeted disruption of TGF-beta1/Smad3 signaling protects against renal tubulointerstitial fibrosis induced by unilateral ureteral obstruction. *J Clin Invest.* 2003;112(10):1486-1494.

28. Wang J, and Pantopoulos K. Regulation of cellular iron metabolism. *Biochem J.* 2011;434(3):365-381.

29. Radoshitzky SR, et al. Transferrin receptor 1 is a cellular receptor for New World haemorrhagic fever arenaviruses. *Nature.* 2007;446(7131):92-96.

30. Ma LJ, and Fogo AB. PAI-1 and kidney fibrosis. *Front Biosci (Landmark Ed).* 2009;14(6):2028-2041.

31. Heaton JH, et al. Cyclic nucleotide regulation of type-1 plasminogen activator-inhibitor mRNA stability in rat hepatoma cells. Identification of cis-acting sequences. *J Biol Chem.* 1998;273(23):14261-14268.

32. Rouland A, et al. Role of apolipoprotein C1 in lipoprotein metabolism, atherosclerosis and diabetes: a systematic review. *Cardiovasc Diabetol.* 2022;21(1):272.

33. Tziastoudi M, et al. The genetic map of diabetic nephropathy: evidence from a systematic review and meta-analysis of genetic association studies. *Clin Kidney J.* 2020;13(5):768-781.

34. Bus P, et al. Apolipoprotein C-I plays a role in the pathogenesis of glomerulosclerosis. *J Pathol.* 2017;241(5):589-599.

35. Zuo Y, et al. Thymosin β4 and its degradation product, Ac-SDKP, are novel reparative factors in renal fibrosis. *Kidney Int.* 2013;84(6):1166-1175.

36. Vasilopoulou E, et al. Loss of endogenous thymosin β(4) accelerates glomerular disease. *Kidney Int.* 2016;90(5):1056-1070.

37. Endele S, et al. C4ORF48, a gene from the Wolf-Hirschhorn syndrome critical region, encodes a putative neuropeptide and is expressed during neocortex and cerebellar development. *Neurogenetics.* 2011;12(2):155-163.
38. Kiyozumi D, et al. A small secreted protein NICOL regulates lumicrine-mediated sperm maturation and male fertility. *Nat Commun.* 2023;14(1):2354.
39. Apodaca G, et al. Receptor-mediated transcytosis of IgA in MDCK cells is via apical recycling endosomes. *J Cell Biol.* 1994;125(1):67-86.
40. Yasumura S, et al. Effects of Heterozygous TfR1 (Transferrin Receptor 1) Deletion in Pathogenesis of Renal Fibrosis in Mice. *Hypertension.* 2020;75(2):413-421.
41. Meng XM, et al. TGF-β: the master regulator of fibrosis. *Nat Rev Nephrol.* 2016;12(6):325-338.
42. Shull MM, et al. Targeted disruption of the mouse transforming growth factor-beta 1 gene results in multifocal inflammatory disease. *Nature.* 1992;359(6397):693-699.
43. Hentze MW, et al. A brave new world of RNA-binding proteins. *Nat Rev Mol Cell Biol.* 2018;19(5):327-341.
44. Kapeli K, et al. Genetic mutations in RNA-binding proteins and their roles in ALS. *Hum Genet.* 2017;136(9):1193-1214.
45. Kang D, et al. RNA-Binding Proteins in Cancer: Functional and Therapeutic Perspectives. *Cancers (Basel).* 2020;12(9):2699.
46. Zheng W, et al. Far Upstream Element-Binding Protein 1 Binds the 3' Untranslated Region of PKD2 and Suppresses Its Translation. *J Am Soc Nephrol.* 2016;27(9):2645-2657.
47. Taguchi K, et al. Cyclin G1 induces maladaptive proximal tubule cell dedifferentiation and renal fibrosis through CDK5 activation. *J Clin Invest.* 2022;132(23):e158096.
48. Jhee JH, et al. CD71 mesangial IgA1 receptor and the progression of IgA nephropathy. *Transl Res.* 2021;230:34-43.

49. Haddad E, et al. Enhanced expression of the CD71 mesangial IgA1 receptor in Berger disease and Henoch-Schönlein nephritis: association between CD71 expression and IgA deposits. *J Am Soc Nephrol.* 2003;14(2):327-337.

50. Goorani S, et al. Kidney Injury by Unilateral Ureteral Obstruction in Mice Lacks Sex Differences. *Kidney Blood Press Res*. 2024;49(1):69-80.

51. Bartos K, Moor MB. FGFR regulator Memo1 is dispensable for FGF23 expression by osteoblasts during folic acid-driven kidney injury. *Physiol Rep*. 2023;11(6):e15650.

Funding:

The National Health and Medical Research Council of Australia APP2003019 (DNP); The National Natural Science Foundation of China No. 81670667 (JL), No. 82300812 (JY), No. 81970599, No. 82170737 and No. 82370707 (WC), No. 81970611 and No. 82170687 (XJ), and No. 81873616 and No. 82170730 (XB); Guangdong Medical University of Provincial and Municipal Construction of Colleges and Universities Project NO. 4SG18001Ga (JL); Guangdong-Hong Kong-Macao-Joint Labs Program from Guangdong Science and Technology No. 2019B121205005 (XY); Guangdong Provincial People's Hospital Research Fund, No. KY012023357 (JL); General project of Natural Science Foundation of Guangdong Province 2019A1515010992 (JF); Key Laboratory of National Health Commission, and Guangdong Provincial Key Laboratory of Nephrology No. 2002B60118 and 2020B1212060028 (WC).

Author Contributions

Conceptualization: JL, DNP

Methodology: JL, DNP, JY, HZ, ANN, NL, HC, XQ, JF, XZ, DW

Investigation: JL, JY, HZ, ANN, NL, HC, AL, XQ, QW, JF, XB, ZY, BG, YM, XZ, DW, YS, XJ, WC, ANC, DNP, XY

Visualization: JL, JY, HZ, NL, HC, AL, XQ, QW, JF, XB, ZY, YS, XJ, WC, DNP, XY

Funding acquisition: JL, DNP, JY, JF, XB, XJ, WC, XY

Project administration: JL, JF

Supervision: JL, DNP, XJ, WC, XY

Writing – original draft: JL, JY, HZ

Writing – review & editing: JL, DNP, AL, JY, HZ, XJ, WC, XY

Competing interests:

J.L., J.Y., and W.C. have filed a patent application: Cf48 is a biomarker for the activity of renal injury and fibrosis and a therapeutic target of kidney disease (Application/Patent No.202210614388.9). Other authors have declared that no competing interests exist.

Data and materials availability:

All data are available in the main text or the supplementary materials.

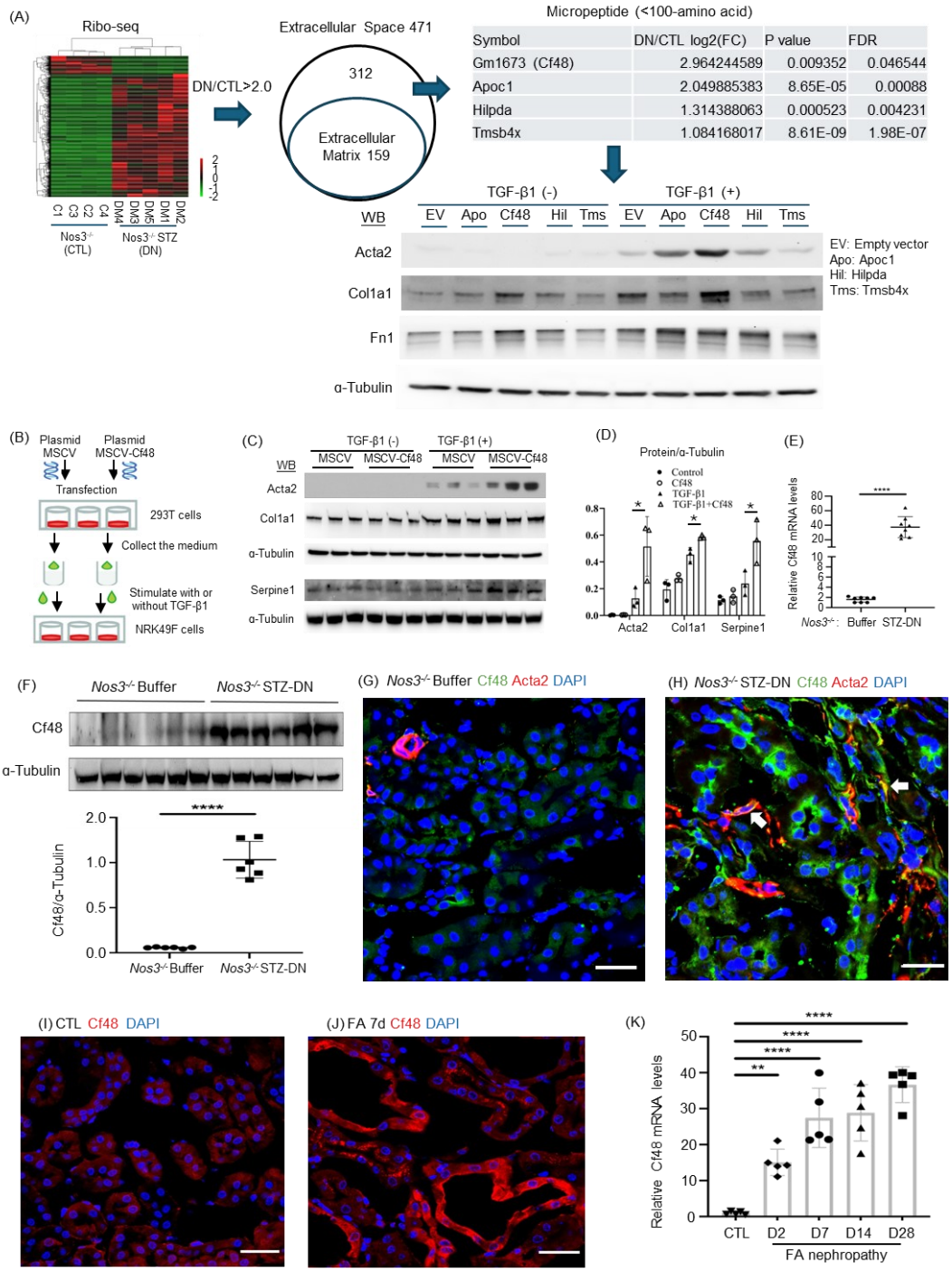

Figure 1. Identification of Gm1673 (C4orf48) as a candidate enhancer of renal fibrosis. (**A**) Flow chart of the screen of kidney tissue from streptozotocin (STZ)-induced diabetic nephropathy (DN) in *Nos3*$^{-/-}$ mice versus age-matched *Nos3*$^{-/-}$ mice control (CTL) mice. Ribosome-sequencing (Ribo-seq) with bioinformatic analysis identified 471 differentially expressed RNAs as candidate extracellular molecules,

including 4 peptides: mouse Gm1673 (C4orf48 in humans, Cf48), Apoc1, Hilpda, and Tmsb4x. Each peptide was overexpressed in NRK49F cells using a retroviral vector, then cells underwent 48 hr with or without TGF-β1 stimulation and were analyzed for Acta2, collagen I and fibronectin expression by Western blotting (WB). (**B-D**) 293T cells were transfected with an empty vector (MSCV) or Cf48 expressing vector (MSCV-Cf48). Cell conditioned medium was collected after 48 h, and used to treat NRK49F cells with or without TGF-β1 stimulation for 48 h. (**C**) WB analysis of Acta2, collagen I and Serpine1 expression, with quantification (**D**). Data are expressed as mean ± SD. One-way ANOVA with Tukey's post-test: *P<0.05. Analysis of Cf48 expression in kidneys at 6-weeks after STZ-induced diabetic nephropathy (DN) in *Nos3*$^{-/-}$ mice versus control buffer treated mice showing: (**E**) RT-qPCR, and (**F**) WB. Student's t-test: ****P<0.0001. Confocal microscopy of Cf48 (green) and Acta2 (red) staining kidney of control *Nos3*$^{-/-}$ (**G**), and *Nos3*$^{-/-}$ DN (**H**). Arrows indicate double labelled Acta2+Cf48+ cells. Analysis of kidney Cf48 expression in day 7 FA nephropathy showing confocal microscopy of Cf48 staining in control (CTL) (**I**) and FA kidneys (**J**), and RT-PCR analysis of Cf48 RNA expression (**K**). Data are expressed as mean ± SD. One-way ANOVA with Tukey's post-test: **P<0.01; ****P<0.0001. Scale bar, 50 μm.

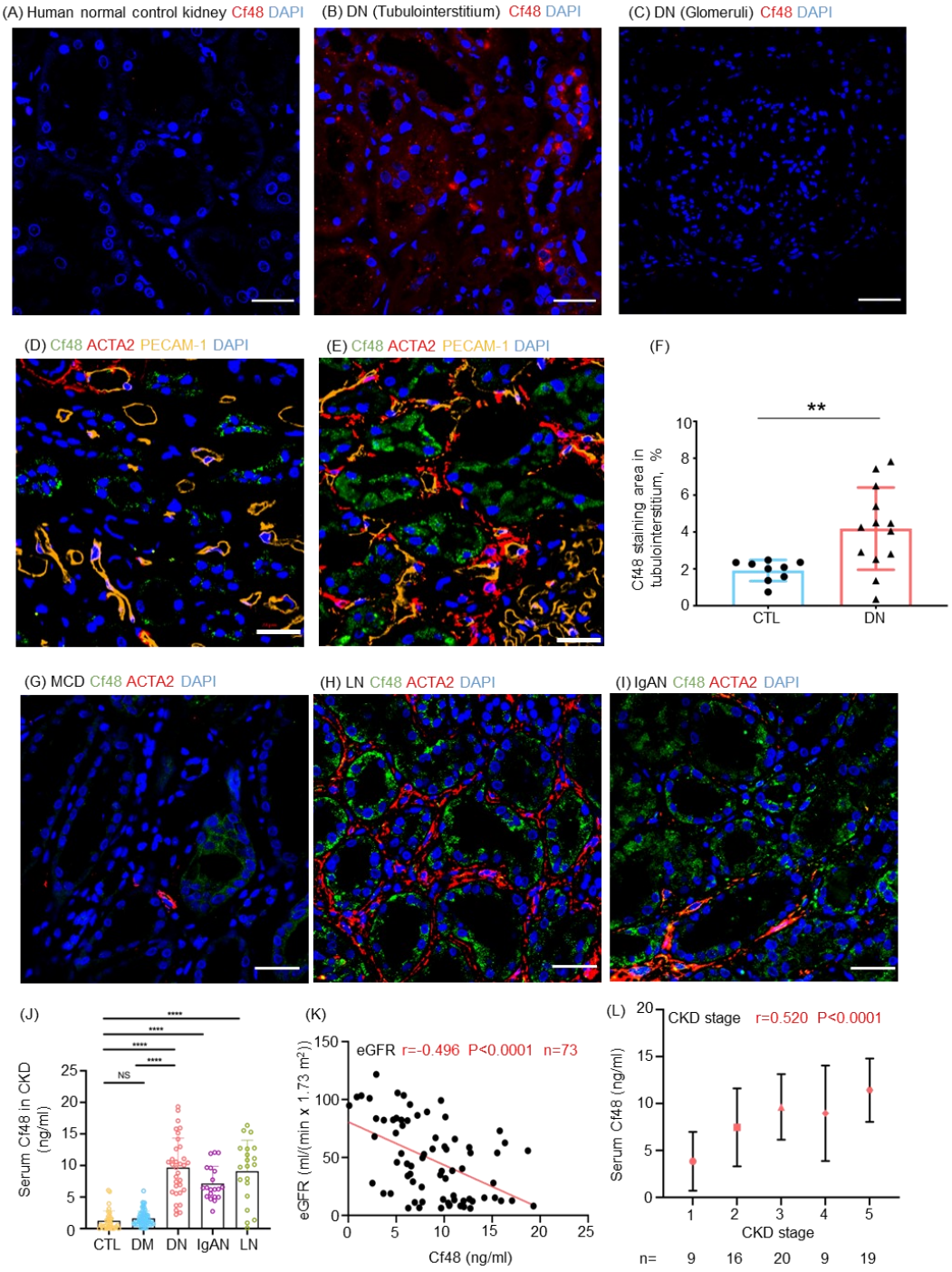

Figure 2. Cf48 expression in human kidney disease. *In situ* hybridization shows a lack of *Cf48* RNA expression in normal control kidney (A), and upregulation of *Cf48* RNA in the tubulointerstitium in diabetic nephropathy (DN) (**B**), but virtually absent in the glomerular compartment in DN (**C**). Confocal microscopy staining of Cf48 (green), ACTA2 (red), PECAM-1(CD31, yellow), and DAPI (blue) in normal control

kidney (**D**) and DN (**E**). Quantitation of the Cf48 staining area (%) in the tubulointerstitium in normal control (CTL) and DN. Student's t-test, **P<0.01 (**F**). Confocal microscopy staining of Cf48 (green), ACTA2 (red), and DAPI (blue) in minimal change disease (MCD) (**G**), lupus nephritis (LN) (**H**), and IgA nephropathy (IgAN) (**I**). (**J**) Serum Cf48 levels in normal healthy controls (CTL), diabetes mellitus without kidney disease (DM), DN, IgAN, and LN. Data are expressed as mean ± SD. One-way ANOVA with Tukey's multiple comparison test: NS, not significant; ****P<0.0001. (**K**) Spearman's correlation between serum Cf48 levels and estimated glomerular filtration rate (eGFR) in DN, LN and IgAN groups. (**L**) Spearman's correlation between serum Cf48 levels and CKD stage in DN, LN and IgAN groups. Scale bar, 50 μm.

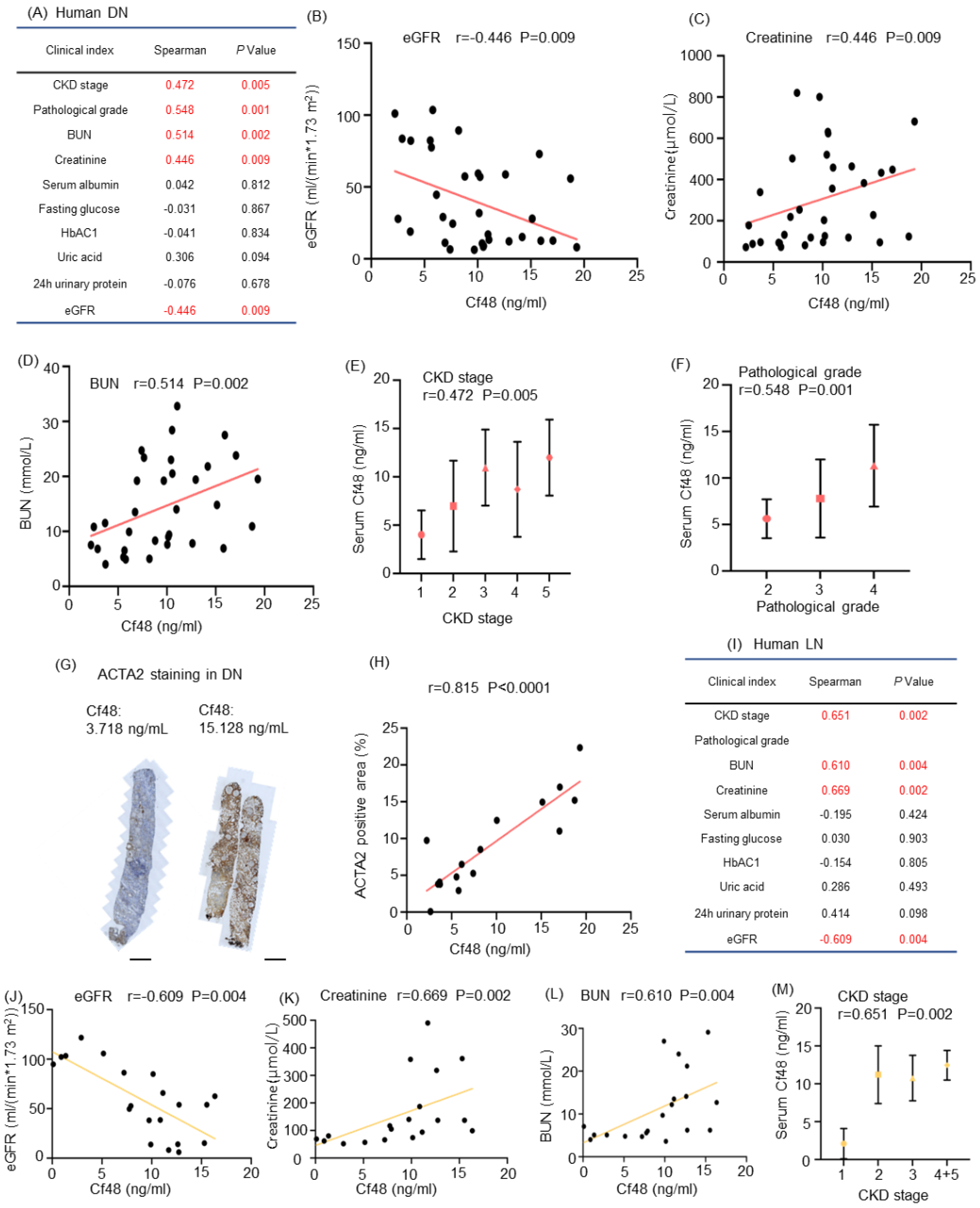

Figure 3. Correlation of serum Cf48 levels with clinical and pathological parameters in human CKD. (**A-H**) Analysis of human diabetic nephropathy (DN) (n=33). (**A**) Correlation table of serum Cf48 levels and various clinical indices. Graphs show correlations between serum Cf48 levels and estimated glomerular filtration rate (eGFR) (**B**), serum creatinine levels (**C**), blood urea nitrogen (BUN) levels (**D**), CKD stage (**E**), and pathological grade (**F**). (**G**) Examples of ACTA2 immunostaining in DN cases with low or high serum Cf48 levels. (**H**) Correlation of

serum Cf48 levels with interstitial area of ACTA2 staining. (**I-M**) Analysis of human lupus nephritis (LN) (n=20). (**I**) Correlation table of serum Cf48 levels and various clinical indices. Graphs show correlations between serum Cf48 levels and eGFR (**J**), serum creatinine levels (**K**), blood urea nitrogen (BUN) levels (**L**), and CKD stage (**M**). Scale bar, 1mm.

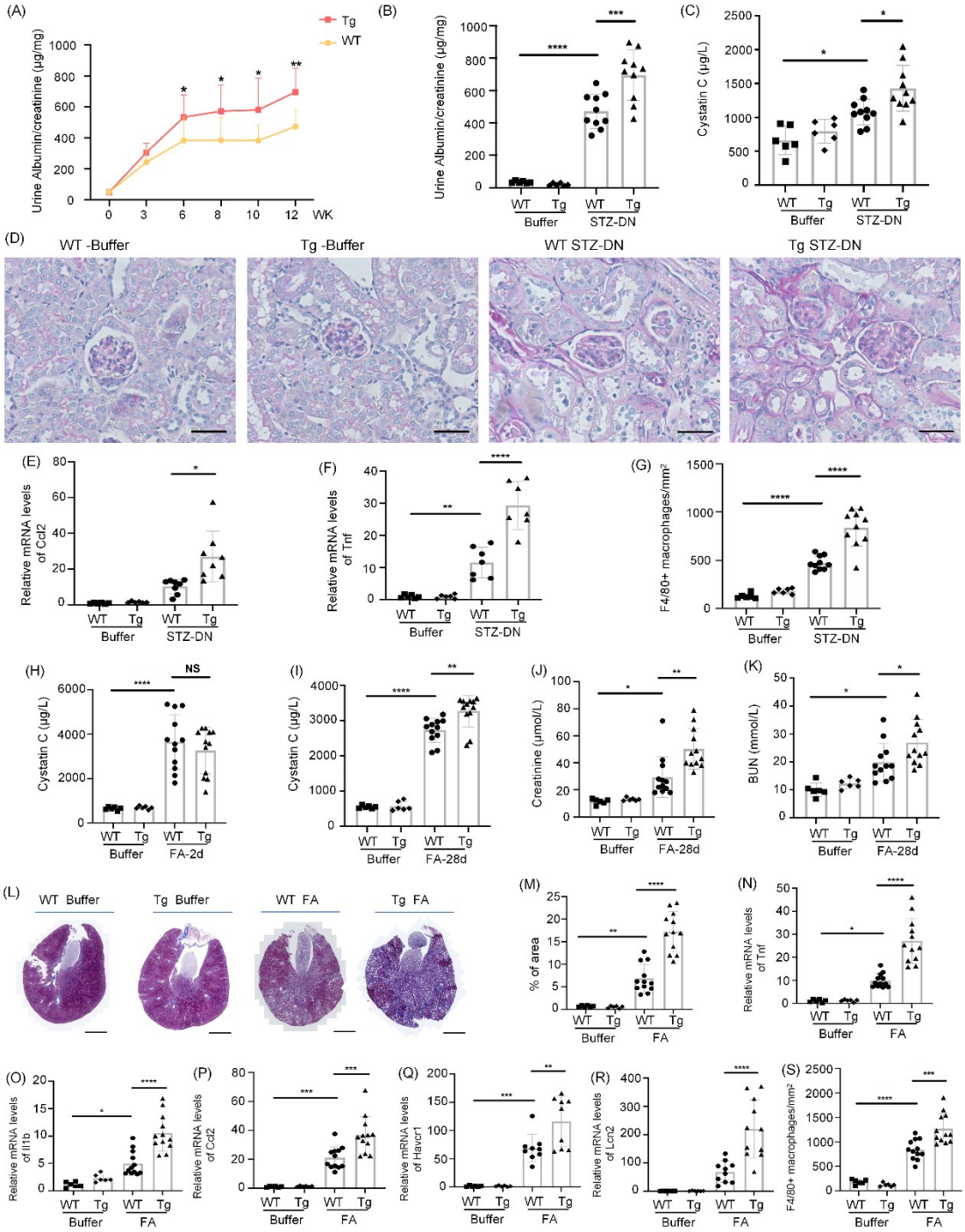

Figure 4. Cf48 overexpression enhances renal fibrosis and inflammation in mouse CKD models. (**A-G**) A 12-week streptozotoxin (STZ)-induced DN model in wild type (WT) and *Cf48* transgenic (Tg) mice with buffer injected mice as non-diabetic controls. (**A**) Time course of the urine albumin/creatinine ratio. Student t-test:

*P<0.05; **P<0.01. (**B**) Urine albumin/creatinine ratio at week 12. (**C**) Serum cystatin C levels. (**D**) PAS staining in 12-week STZ- DN or buffer-treated WT or Cf48 Tg mouse kidneys. Scale bar, 50 μm. RT-qPCR analysis of *Ccl2* (**E**) and *Tnf* (**F**) mRNA levels. (**G**) Number of F4/80+ macrophages scored from immunostaining. (**H-S**) Day 2 and 28 folic acid nephropathy (FAN) in WT and *Cf48* Tg mice with buffer injected mice as controls. (**H**) Serum cystatin C levels on day 2 FAN. Serum levels of: (**I**) cystatin C; (**J**) creatinine, and; (**K**) blood urea nitrogen (BUN), on day 28 FAN. Representative while kidney cross-sections (**L**, scale bar 1 mm) and quantification (**M**) of interstitial collagen deposition in Masson trichrome stained kidneys on day 28 FAN. RT-qPCR analysis of kidney mRNA levels of: (**N**) *Tnf*; (**O**) *Il1b*: (**P**) *Ccl2*; (**Q**) *Kim1/Havcr1*, and; (**R**) *Ngal/Lcn2*, on day 28 FAN. (**S**) Number of F4/80+ macrophages scored from immunostaining. Data are expressed as mean ± SD. One-way ANOVA with Tukey's multiple comparison test: *P<0.05; **P<0.01; ***P<0.001; ****P<0.0001.

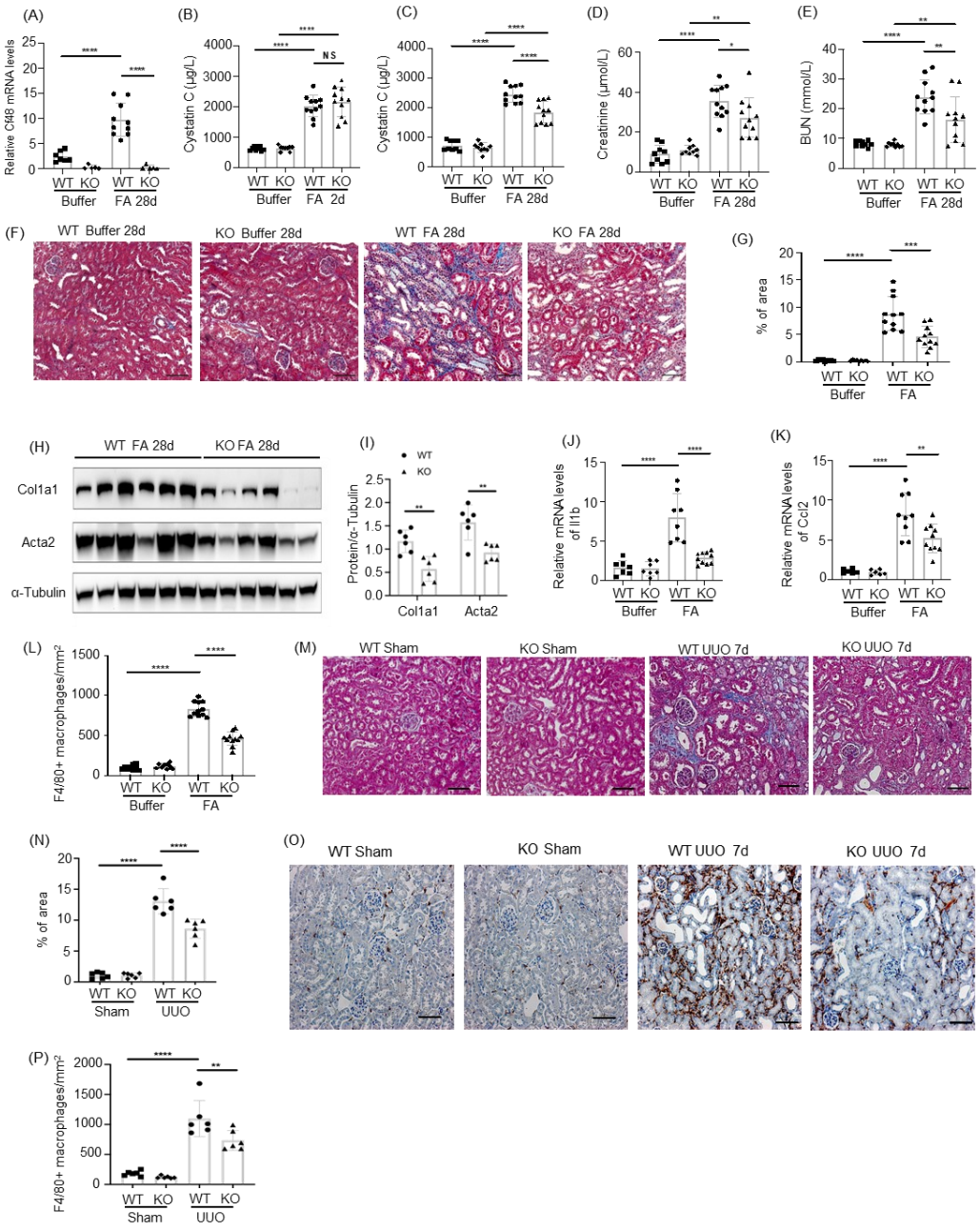

Figure 5. Cf48 deficiency suppresses renal fibrosis in mouse CKD models. Day 2 and 28 folic acid nephropathy (FAN) in WT and *Cf48* KO mice with buffer injected mice as controls. (**A**) Kidney *Cf48* mRNA levels on day 28 FAN or buffer control. (**B**) Serum cystatin C levels on day 2 FAN. Serum levels of: (**C**) cystatin C; (**D**) creatinine, and; (**E**) blood urea nitrogen (BUN), on day 28 FAN. (**F**) Masson

trichrome staining of kidney sections on day 28 FAN, with (**G**) quantification of interstitial collagen deposition. (**H**) Western blot of kidney lysates for collagen I and Acta2 on day 28 FAN, with (**I**) quantification of bands compared to the α-tubulin control. RT-qPCR analysis of kidney mRNA levels of: (**J**) *Il1b*, and; (**K**) *Ccl2*, on day 28 FAN. Quantification of F4/80 positive staining cells in the day 28 FAN model (**L**). WT and Cf48 KO mice were also compared in a day 7 unilateral ureteral obstruction (UUO) model with sham surgery controls. (**M**) Masson trichrome staining of day 7 UUO and sham controls. (**N**) Quantification of Masson trichrome stain interstitial collagen. (**O**) F4/80 immunostaining in day 7 UUO and sham controls. Quantification of F4/80 positive staining cells in the day 7 UUO model (**P**). Data are expressed as mean ± SD. One-way ANOVA with Tukey's multiple comparison test: NS, not significant; *P<0.05; **P<0.01; ***P<0.001; ****P<0.0001. Scale bar, 50 μm.

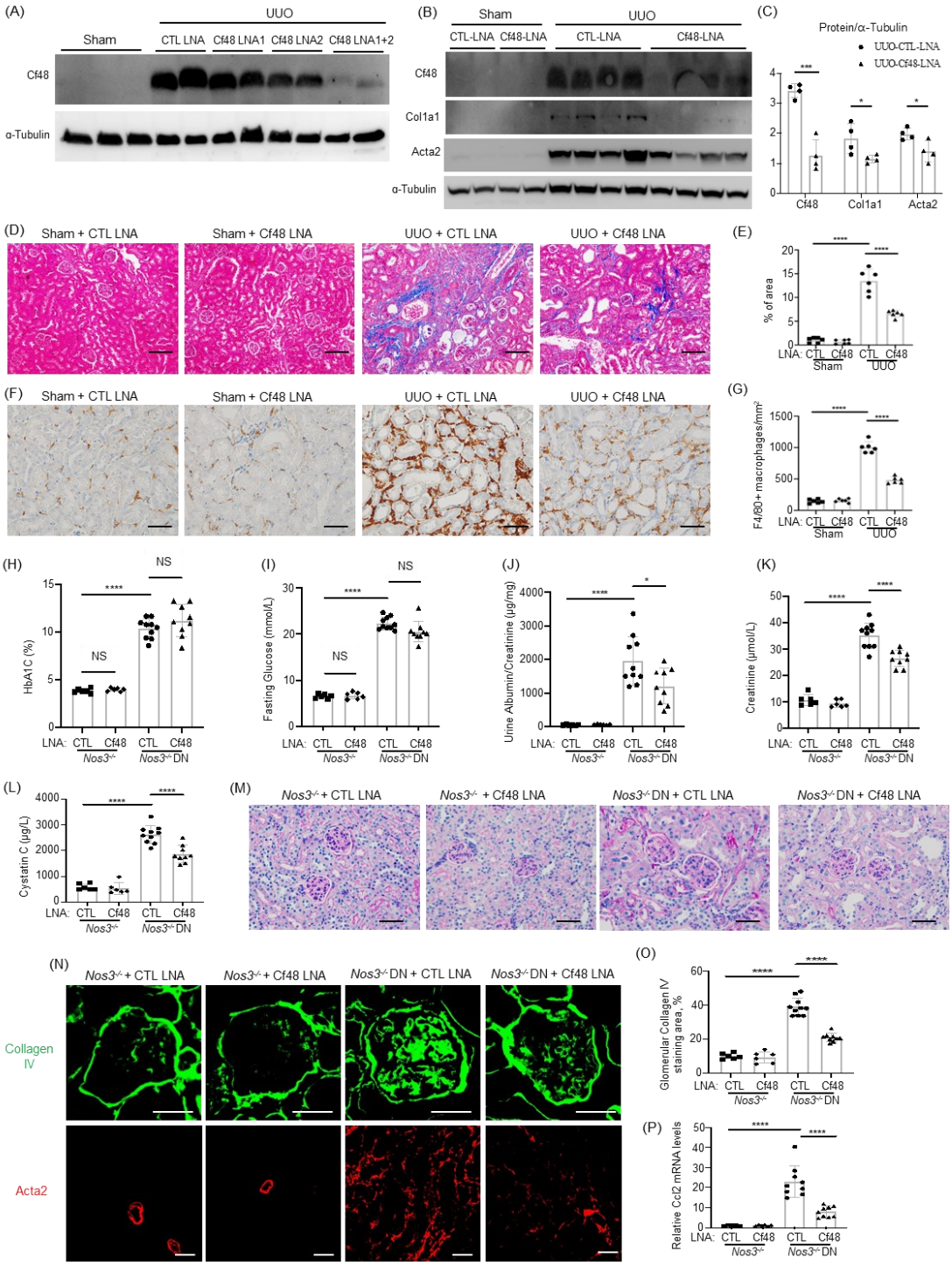
(A)
Sham
UUO
CTL LNA
Cf48 LNA1
Cf48 LNA2
Cf48 LNA1+2
Cf48
α-Tubulin
(B)
Sham
UUO
CTL-LNA
Cf48-LNA
CTL-LNA
Cf48-LNA
Cf48
Col1a1
Acta2
α-Tubulin
(C)
Protein/α-Tubulin
UUO-CTL-LNA
UUO-Cf48-LNA
Cf48
Col1a1
Acta2
(D)
Sham + CTL LNA
Sham + Cf48 LNA
UUO + CTL LNA
UUO + Cf48 LNA
(E)
% of area
LNA: CTL Cf48 CTL Cf48
Sham
UUO
(F)
Sham + CTL LNA
Sham + Cf48 LNA
UUO + CTL LNA
UUO + Cf48 LNA
(G)
F4/80+ macrophages/mm²
LNA: CTL Cf48 CTL Cf48
Sham
UUO
(H)
HbA1C (%)
NS
LNA: CTL Cf48 CTL Cf48
Nos3-/-
Nos3-/- DN
(I)
Fasting Glucose (mmol/L)
NS
LNA: CTL Cf48 CTL Cf48
Nos3-/-
Nos3-/- DN
(J)
Urine Albumin/Creatinine (μg/mg)
LNA: CTL Cf48 CTL Cf48
Nos3-/-
Nos3-/- DN
(K)
Creatinine (μmol/L)
LNA: CTL Cf48 CTL Cf48
Nos3-/-
Nos3-/- DN
(L)
Cystatin C (μg/L)
LNA: CTL Cf48 CTL Cf48
Nos3-/-
Nos3-/- DN
(M)
Nos3-/- + CTL LNA
Nos3-/- + Cf48 LNA
Nos3-/- DN + CTL LNA
Nos3-/- DN + Cf48 LNA
(N)
Nos3-/- + CTL LNA
Nos3-/- + Cf48 LNA
Nos3-/- DN + CTL LNA
Nos3-/- DN + Cf48 LNA
Collagen IV
Acta2
(O)
Glomerular Collagen IV staining area, %
LNA: CTL Cf48 CTL Cf48
Nos3-/-
Nos3-/- DN
(P)
Relative Ccl2 mRNA levels
LNA: CTL Cf48 CTL Cf48
Nos3-/-
Nos3-/- DN

Figure 6. Cf48 LNA administration reduces renal fibrosis and inflammation in mouse CKD models. (**A**) Mice received control 10 mg/kg control LNA (CTL LNA), 10 mg/kg Cf48 LNA 1, 10 mg/kg Cf48 LNA2, or 5 mg/kg Cf48 LNA1 + 5 mg/kg Cf48 LNA2 combined treatment on days 1 and 4 after completing UUO surgery, with mice killed on day 7. Sham operated mice were controls. Western blot of Cf48 expression in day 7 UUO and sham groups. (**B-G**) Day 7 UUO with 5 mg/kg Cf48 LNA1 + 5 mg/kg Cf48 LNA2 (termed Cf48 LNA) or CTL LNA treatment, with sham controls. (**B**) Western blot of kidney Cf48, collagen I and Acta2 expression, with quantification of blots in (**C**). (**D**) Masson trichrome staining, with quantification of interstitial collagen staining (**E**). (**F**) Immunostaining of F4/80+ macrophages, with quantification (**G**). (**H-P**) *Nos3*$^{-/-}$ mice were treated weekly with Cf48 LNA or CTL LNA from 3 weeks after STZ (or buffer administration) until being killed on week 8. (**H**) Glycated haemoglobin A1c levels (HbA1c). (**I**) Fasting blood glucose levels. (**J**) Urinary albumin to creatinine levels. (**K**) Serum creatinine levels. (**L**) Serum cystatin C levels. (**M**) PAS staining of kidney sections. (**N**) Immunofluorescence staining of collagen IV and Acta2. (O) Quantification of percentages of glomerular Collagen IV staining. (**P**) RT-qPCR analysis of kidney *Ccl2* mRNA levels. Data are expressed as mean ± SD. One-way ANOVA with Tukey's multiple comparisons test: NS, not significant; *P<0.05; ***P<0.001; ****P<0.0001.

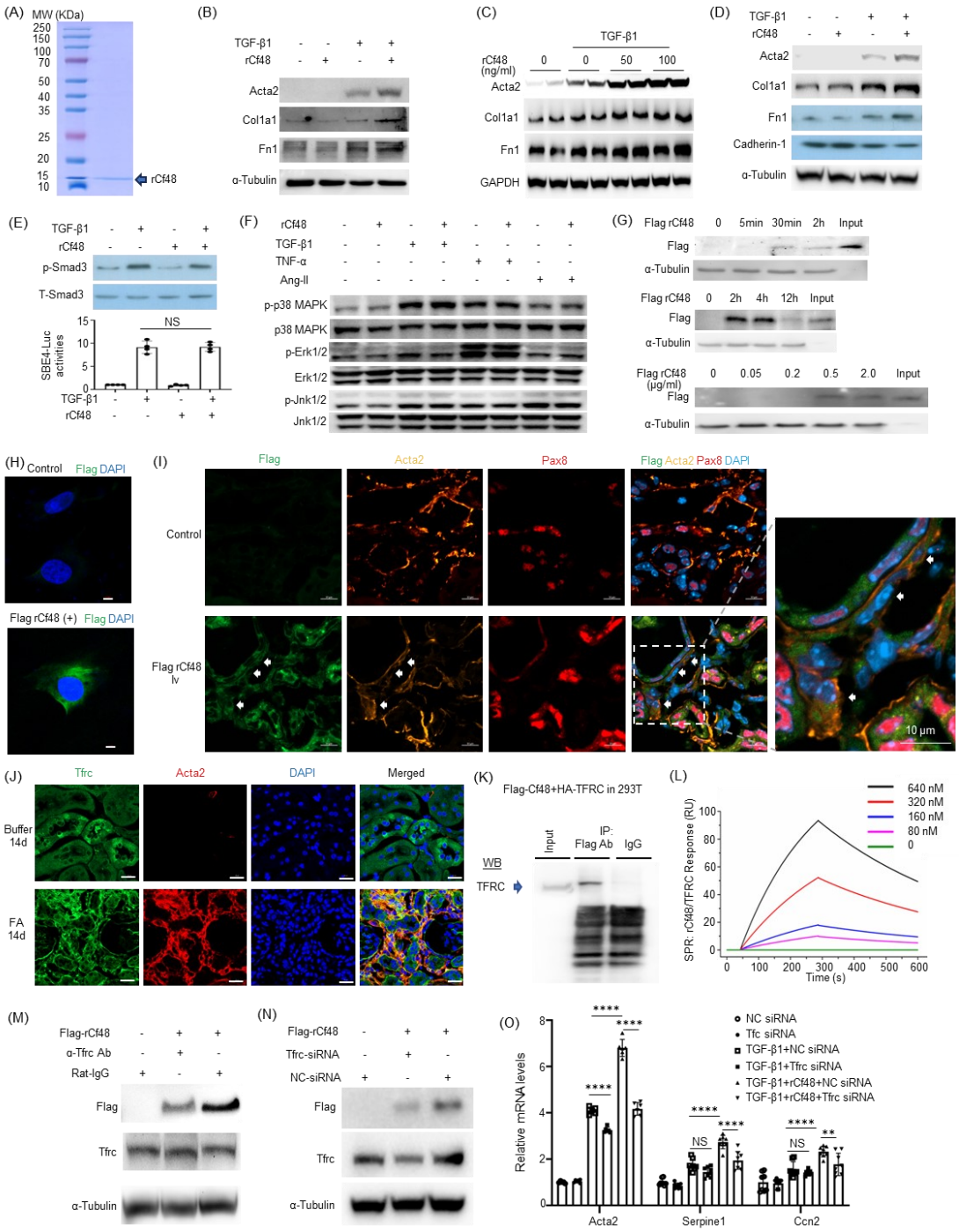

Figure 7. **Cf48 enhances the TGF-β1-induced fibrotic response via the transferrin receptor (TFRC).** (**A**) Characterization of recombinant mouse Cf48 (rCf48) lacking the signal peptide (i.e. secreted form) via SDS-PAGE. Stimulation of NRK49F cells (**B and C**) or NRK52E cells (**D**) with rCf48 ± TGF-β1 for 48 h. Western blots (WB) show Acta2, collagen I, fibronectin, and cadherin-1 expression.

(**E**) **Upper panel:** NRK49F cells were stimulated for 30 min with rCf48 ± TGF-β1 and expression of total Smad3 (T-Smad3) and c-terminal phosphorylation of Smad3 (p-Smad3) shown by WB. **Lower panel**: SBE4-luciferase activity assessed in 293T cells at 15 h after stimulation with rCf48 ± TGF-β1. (**F**) WB analysis of phosphorylation of p38 MAPK, ERK1/2 and JNK at 30 min after stimulation of NRK49F cells with rCf48± TGF-β1, TNF-α, or angiotensin II (ATII). (**G**) NRK49F cells were cultured with flag-tagged rCf48 for different times (top two blots), or with different doses of flag-tagged rCf48 for 2 h (bottom blot). Uptake of flag-tagged rCf48 was assessed by WB. (**H**) Confocal microscopy shows uptake of flag-tagged rCf48 (green) at 2 h after addition to NRK49F cells. Scale bar, 5 μm. (**I**) Confocal microscopy mouse kidney 5 min after tail vein injection of 200 μg of flag-tagged rCf48 (green) in day 14 FAN. Arrows indicate myofibroblasts double stained for flag and Acta2 (yellow). Scale bar, 10 μm. (**J**) Confocal microscopy showing Tfrc expression in renal tubular epithelial cells and myofibroblasts in buffer control mice and on day 14 FAN. Scale bar, 20 μm. (**K**) Immunoprecipitation/WB shows an interaction between flag-tagged Cf48 and HA-tagged TFRC after both were overexpressed in 293T cells. (**L**) Surface plasmon resonance (SPR) shows an interaction between rCf48 and recombinant TFRC. (**M and N**) WB shows that uptake of flag-tagged rCf48 after a 2 h incubation with NRK49F cells can be substantially reduced by pretreatment with a neutralizing anti-Tfrc antibody (versus rat IgG control) (**M**), or by pretreatment with *Tfrc* siRNA (versus control siRNA) (**N**). (**O**) RT-qPCR analysis of *Acta2*, *Ccn2* and *Serpine1* mRNA levels 6 h after flag-tagged

rCf48 stimulation in NRK49F cells pretreated with control or *Tfrc* siRNA. Data are expressed as mean ± SD. One-way ANOVA with Tukey's multiple comparisons test: NS, not significant; **P<0.01; ****P<0.0001.

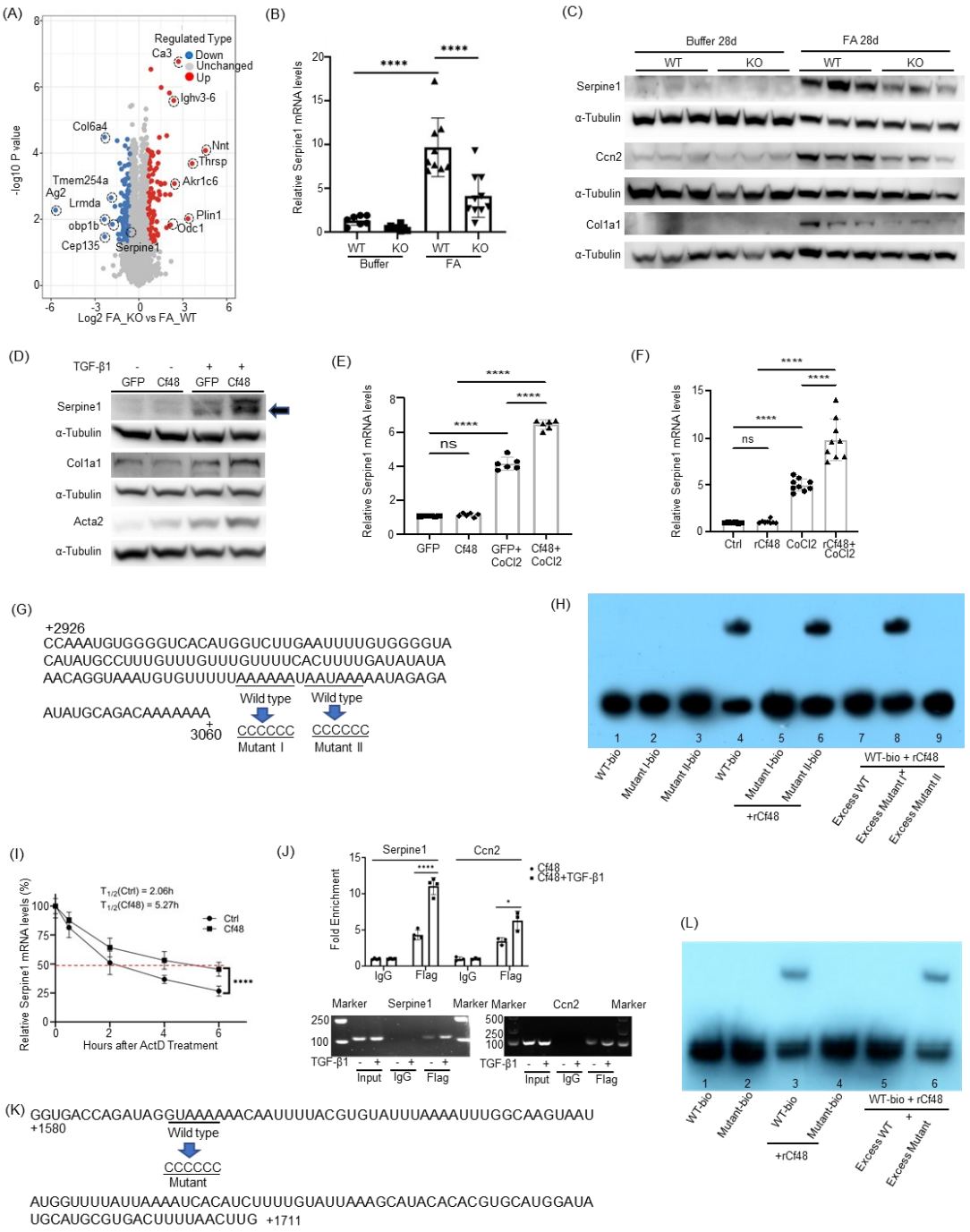

Figure 8. **Cf48 is a mRNA-binding protein that regulates mRNA stability**. (**A**) Volcano plot of changes in protein abundance in day 28 folic acid-induced nephropathy (FAN) in WT or *Cf48* KO kidneys. Average protein expression ratio of three replicates (log 2 transformed) between FA KO versus FA WT. Different treatment groups were plotted against P-value by t-test (-log 10 transformed). The cut-

off of P = 0.05 and 2-fold change are marked by blue and red dots, respectively. (**B**) RT-qPCR analysis of *Serpine1* mRNA levels in day 28 FAN or buffer-treated control WT or *Cf48* KO kidneys. Data are expressed as mean ± SD. One-way ANOVA with Tukey's multiple comparisons test: ****P < 0.0001. (**C**) Western blot (WB) analysis of Serpine1, Ccn2 and collagen I protein levels in day 28 FAN and control WT and KO kidneys. (**D and E**) NRK49F cells were transduced with retroviral vector PMSCV-Cf48-IRES-GFP or PMSCV-IRES-GFP. GFP-positive cells were sorted by FACS and then cultured with or without TGF-β1 for 2 days for WB analysis (**D**), or cultured with and without CoCl2 for 6 h and *Serpine1* mRNA levels were assessed by RT-qPCR (**E**). (**F**) NRK49F cells were cultured with or without rCf48 ± CoCl2 for 6 hrs and *Serpine1* mRNA levels were assessed by RT-qPCR. (**G**) Nucleotide sequence of *Serpine1* mRNA from position 2926–3060 with potential binding sites and their mutated versions shown. (**H**) RNA Electrophoretic Binding Assay (RNA-EMSA) analysis of binding interactions between biotin-labelled *Serpine1* probes and the rCf48 peptide. Lanes are: (1) Bio-labeled wild-type (WT-bio) probe; (2) mutant I-bio; (3) mutant II-bio; (4) WT-bio + rCf48; (5) mutant I-bio + rCf48; (6) mutant II-bio + rCf48; (7) WT-bio + excess WT + rCf48; (8) WT-bio + excess mutant I + rCf48; (9) WT-bio + excess mutant II + rCf48. (**I**) NRK49F cells were stimulated with TGF-β1 for 6 h, then actinomycin D was added and decay of *Serpine1* mRNA in the presence or absence of rCf48 was measured by RT-qPCR. RT-qPCR demonstrated levels of *Serpine1* mRNA after TGF-β1± rCf48 treatment. Unpaired student's t-test, ****P<0.0001. (**J**) Upper panel, RIP and RT-qPCR identified rCf48 binding mRNAs:

Serpine1 and *Ccn2*, while TGF-β1 increased the binding of Cf48 to *Serpine1* and *Ccn2* mRNAs in NRK49F cells. Data are expressed as mean ± SD. Student's t-test. *P<0.05; ****P<0.0001. Lower panel, End-products of RIP-RT-qPCR *Serpine1* and *Ccn2* were visualized in agarose gel. (**K**). Nucleotide sequence of *Acta2* mRNA from position 1580–1711 with the potential Cf48 binding site, and its mutation. (**L**) RNA-EMSA for interactions between *Acta2* probes and the rCf48 peptide. Lanes are: (1) biotin-labeled wild-type (WT-bio) probe; (2) mutant-bio; (3) WT-bio + rCf48; (4) mutant-bio + rCf48; (5) WT-bio + excess WT + rCf48; (6) WT-bio + excess mutant + rCf48.